Journal of Catalysis **184,** 87–104 (1999)
Article ID jcat.1999.2452, available online at http://www.idealibrary.com on IDEAL®

Transient FTIR Studies of the Reaction Pathway for *n*-Butane Selective Oxidiation over Vanadyl Pyrophosphate

Zhi-Yang Xue and G. L. Schrader

Department of Chemical Engineering and Ames Laboratory-USDOE, Iowa State University, Ames, Iowa 50011

Received July 30, 1998; revised February 12, 1999; accepted February 12, 1999

New information has been provided about the reaction pathway for *n*-butane partial oxidation to maleic anhydride over vanadyl pyrophosphate (VPO) catalysts using FTIR spectroscopy under transient conditions. Adsorption studies of *n*-butane, 1,3-butadiene, and related oxygenates were performed to gain information about reaction intermediates. *n*-Butane was found to adsorb on the VPO catalyst to form olefinic species at low temperatures. Unsaturated, noncyclic carbonyl species were determined to be precursors to maleic anhydride. © 1999 Academic Press

Key Words: ***n*-butane oxidation; VPO catalysts; transient FTIR; adsorbed intermediates.**

INTRODUCTION

The selective oxidation of *n*-butane to maleic anhydride over vanadium phosphorus oxide catalysts (VPO) has been studied for more than 20 years (1–4). Commercial technologies using fixed bed reactors, fluidized bed reactors, and more recently a circulating fluidized bed reactor have been developed (2). Despite the commercial success of this processing route, many aspects of the reaction mechanism are not well understood.

Only very little byproducts other than carbon dioxide are produced under commercial reaction conditions (3). In laboratory studies, however, butene, 1,3-butadiene, furan, crotonaldehyde, and methyl vinyl ketone, etc. have been reported to be present in reactor effluents (4, 5). Several general reaction pathways have been proposed based on these observations (3). A frequently cited reaction scheme involves the following steps (2–4):

n-butane → butenes → 1,3-butadiene → 2,5-dihydrofuran → furan → 2(5*H*)-furanone → maleic anhydride.

Typically, *n*-butane oxidative dehydrogenation to butenes has been suggested to be the rate-limiting step. Oxidation of the butene isomers generates 1,3-butadiene which cyclizes upon oxygen insertion to form 2,5-dihydrofuran. According to this reaction pathway, furan is produced by further allylic oxidation. Oxygen insertion at the α-position of the furan ring generates 2(5*H*)-furanone; additional oxygen insertion at the α-position of 2(5*H*)-furanone results in production of maleic anhydride. Noncyclic oxygenates, such as methyl vinyl ketone and crotonaldehyde, can also be formed but are believed to undergo complete oxidation (2–4).

This reaction pathway postulates the formation of cyclic oxygenates; however, other reaction intermediates have also been proposed which do not involve the formation of furan-related cyclic species. Zhang-Lin *et al.* (6, 7) studied the oxidation of *n*-butane, 1,3-butadiene, furan, and maleic anhydride on various VPO phases. Maleic anhydride was observed to be formed from *n*-butane, while only a small amount of maleic anhydride was obtained from of 1,3-butadiene and furan molecular intermediates (6). Zhang-Lin *et al.* proposed an "alkoxide route" for maleic anhydride formation, in which adsorbed noncyclic species were the precursors to maleic anhydride (7). Ziólkowski *et al.* (8) examined the energetics and geometries of favorable pathways for *n*-butane and 1-butene oxidation on the (100) face of $(VO)_2P_2O_7$. Analysis of the heats of reaction for each possible reaction step on the surface suggested that the intermediates in *n*-butane oxidation were noncyclic species anchored on the surface through $C_{terminal}$–$O_{surface}$ bonds.

In situ spectroscopic investigations of surface species have provided important insights into the reaction intermediates for these reaction pathways. Fourier transform infrared (FTIR) spectroscopy is one of a few techniques capable of detecting surface compounds in heterogeneous reaction systems under reaction conditions (9). Several groups have performed *in situ* FTIR studies to investigate *n*-butane oxidation on vanadium oxide-based catalysts (10–19). Due to the complexity of the reaction on VPO catalysts, however, it is unlikely that surface intermediates can be identified by FTIR studies using only *n*-butane. The general approach has been to perform FTIR studies for the adsorption of compounds expected to be related to surface species, such as 1-butene, 1,3-butadiene, furan, maleic anhydride, etc. Previous studies have also emphasized steady-state adsorption or reaction conditions. These approaches have come under criticism in recent years, and with current

0021-9517/99 $30.00

TABLE 1

Common IR Bands (cm^{-1}) Observed in C_4 Hydrocarbon Oxidation on VPO and Their Assignments

Position	Assignment	Remarks
1850	$\nu_{s\ C=O}$ of maleic anhydride	Weak shoulder band; reported in the study of *n*-butane (10), 1-butene (10, 18), 1,3-butadiene (19), furan (16, 18), 2,5-dihydrofuran (18), 2(5*H*)-furanone (16).
1775	$\nu_{as\ C=O}$ of maleic anhydride	Strong band, reported in most of the studies; associated bands at 1795 cm^{-1} and 1765 cm^{-1} found in furan adsorption (15, 17) and 2(5*H*)-furanone adsorption (16) were attributed to 2(5*H*)-furanone.
1715 ± 20	$\nu_{C=O}$ stretching vibration	Reported in the study of *n*-butane (10, 18), 1-butene (11, 18), 1,3-butadiene (19), 2,5-dihydrofuran (18), furan (16, 18), 2(5*H*)-furanone (16), maleic anhydride (12, 16), and maleic acid (12); assigned to carbonyl stretching of 2(5*H*)-furanone (18, 19), maleic acid (10), aldehyde species (16), or furan (15).
1620 ± 30	$\nu_{C=C}$ stretching vibration	Reported in most of the adsorption studies (10–19); attributed to unsaturated surface species; adsorbed water (13) and carbon oxide (14) also have bands around 1620 cm^{-1}.
1560 ± 20	$\nu_{as\ COO^-}$	Reported in 1,3-butadiene (15, 19), furan (17), and maleic anhydride (15, 16), acetic anhydride (14) oxidation; attributed to surface carboxylate species together with the band near 1430 cm^{-1} (14, 17, 19).
1490	Ring vibration of furan	Reported in 1,3-butadiene oxidation (18) and furan adsorption (16); attributed to furan.
1460	Ring vibration of furan	Attributed to surface-bound furan (16, 18).
1430 ± 20	$\nu_{s\ COO^-}$	Attributed to surface carboxylate species together with the band at 1560 cm^{-1} (14, 17, 19).

advances in instrumentation, transient FTIR studies have now become possible.

In our previous studies (10, 11), *in situ* FTIR studies of *n*-butane, 1-butene, 1,3-butadiene oxidation on VPO catalysts were conducted under steady state reaction conditions (1.5% hydrocarbon in air at various temperatures). In all cases, bands at 1845 and 1775 cm^{-1} (due to maleic anhydride) and a band near 1720 cm^{-1} were observed. The later was attributed to maleic acid. Using additional information gained in adsorption studies of crotyl alcohol, maleic acid, crotonic acid, and maleic anhydride, a reaction scheme for 1,3-butadiene oxidation was proposed which involved an unspecified peroxide intermediate species (12).

Puttock and Rochester (13) demonstrated the presence of both Lewis and Brønsted acid sites on the catalyst surface by adsorption of water and pyridine. They further conducted infrared studies of the adsorption of carbon monoxide, carbon dioxide, acetic acid, acetic anhydride, 1-butene, 1,3-butadiene, furan, and maleic anhydride. Many spectral features were attributed to the interactions between acidic sites and adsorbates (14, 15).

Baerns and colleagues (16, 17) investigated the adsorption of 1-butene, 1,3-butadiene, furan, 2(5*H*)-furanone, and maleic anhydride on supported VPO catalysts. An adsorption mode for each adsorbate was proposed. Their analysis favored the argument that furan and 2(5*H*)-furanone retained their ring structure and were directly oxidized to maleic anhydride.

Busca and Centi (18) studied *n*-butane adsorption on the surface of $(VO)_2P_2O_7$. In addition to major bands at 1780 and 1620 cm^{-1}, a shoulder band at 1720–1710 cm^{-1} was reported which was attributed to a 2(5*H*)-furanone-like (lactone) species. Studies of the adsorption of 1-butene, furan, and dihydrofuran were also performed. A reaction scheme was proposed in which furan and 2(5*H*)-furanone were the major intermediates. Later, Busca *et al.* (19) studied 1,3-butadiene adsorption of V_2O_5–TiO_2, and the results suggested the existence of similar reaction intermediates.

Table 1 summaries the observed IR bands and their assignments as reported in these studies (10–19). Bands at 1850 and 1775 cm^{-1} have been used to confirm maleic anhydride formation by oxidation of *n*-butane and other hydrocarbons. Detection of bands near 1715 and 1620 cm^{-1} has also been reported, but their assignment has been less clear. Several possible intermediates, such as surface-bound furan or lactones, have been suggested. In general, the observation and/or interpretation of the spectra has not been consistent among the researchers working in this area, and a convincing reaction pathway has not been developed from the FTIR studies.

In our current research, transient operation techniques including pulse reaction studies and reactant feed cycling have been utilized to induce a departure from steady state operation. These techniques provide an opportunity to explore the reactivity of intermediates and the surface species. Computer simulations have demonstrated that the concentration of surface species under transient operation conditions can be significantly different from that under steady state conditions (20). Therefore, transient IR studies may reveal surface species that are difficult to detect under steady state conditions, such as reaction intermediates which are transformed very rapidly.

EXPERIMENTAL PROCEDURE

Catalyst Preparation and Characterization

The current study used an activated vanadyl pyrophosphate (VPO) catalyst prepared in an organic medium by DuPont (21). The catalyst was prepared by reacting vanadium pentoxide and anhydrous phosphoric acid in

isobutanol and benzyl alcohol. Following the reaction, $VO(HPO_4) \cdot 0.5H_2O$ was precipitated and dried at 100°C. Calcination was performed at 400°C in a N_2–O_2 flow, and the catalyst was activated in a reaction atmosphere at 450°C. Laser Raman, XRD, and infrared spectroscopic characterization revealed that only the vanadyl pyrophosphate phase, $(VO)_2P_2O_7$, was present. The surface area of the catalyst as measured by BET methods was 23 m^2/g.

Catalyst Wafer Preparation and Pretreatment

Polished stainless steel dies were used to press the catalyst powder under a load of 15,000 lb. The resulting catalyst wafer had a diameter of 20 mm, a thickness of 0.1 mm (or less), and a weight of about 50 mg. The catalyst wafer was transferred to a sample holder and placed in the FTIR cell (Fig. 1). Unless indicated by the catalyst pretreatment procedure, wafers were exposed to a nitrogen flow (50 ml/s) at 300°C for 4 h in the FTIR cell. Bands due to adsorbed water (near 1620 cm^{-1} and 3600–3100 cm^{-1}) were largely removed by this procedure.

Fourier Transform Infrared Spectrometer

A Nicolet Model 60-SX FTIR spectrometer was used in these studies. Typically 100 scans were collected at 4 cm^{-1} resolution in about 40 s. For the reaction studies reported here, the time that elapsed between individual spectral acquisitions was 1 min. For the adsorption studies, the time intervals were usually longer. Unless indicated, the spectrum of the pretreated catalyst at the given temperature has been subtracted for spectra presented in this paper. Since the transient studies did not alter the structure of the catalyst, spectral bands were due to the adsorbed or gas-phase species.

FTIR Cell

The design of FTIR cell is shown in Fig. 1. The cell body was constructed from a stainless steel cylinder 40 mm in length with four Swagelok 1/8″ fittings welded 90° apart. The top and bottom fittings were the gas inlet and outlet, respectively; the third fitting was connected to a vacuum line. The fourth fitting allowed the insertion of a 0.040″ thermocouple (Omega Engineering) close to the catalyst surface. At the center of the cell chamber, a ring groove tightly held the stainless steel catalyst sample holder. Two 38 mm × 6 mm KBr windows (International Crystal Laboratories) were used as primary windows. Two 25.2 mm × 5 mm KBr windows were used as secondary windows. Brass end caps pressed the KBr windows against the window mounts which were constructed from Macor machinable glass ceramic (Technical Products). Kalrez O-rings (DuPount Dow Elastormers) were used to seal the windows. The optical path length between inner surfaces of the secondary windows was 20 mm. The cell was heated by

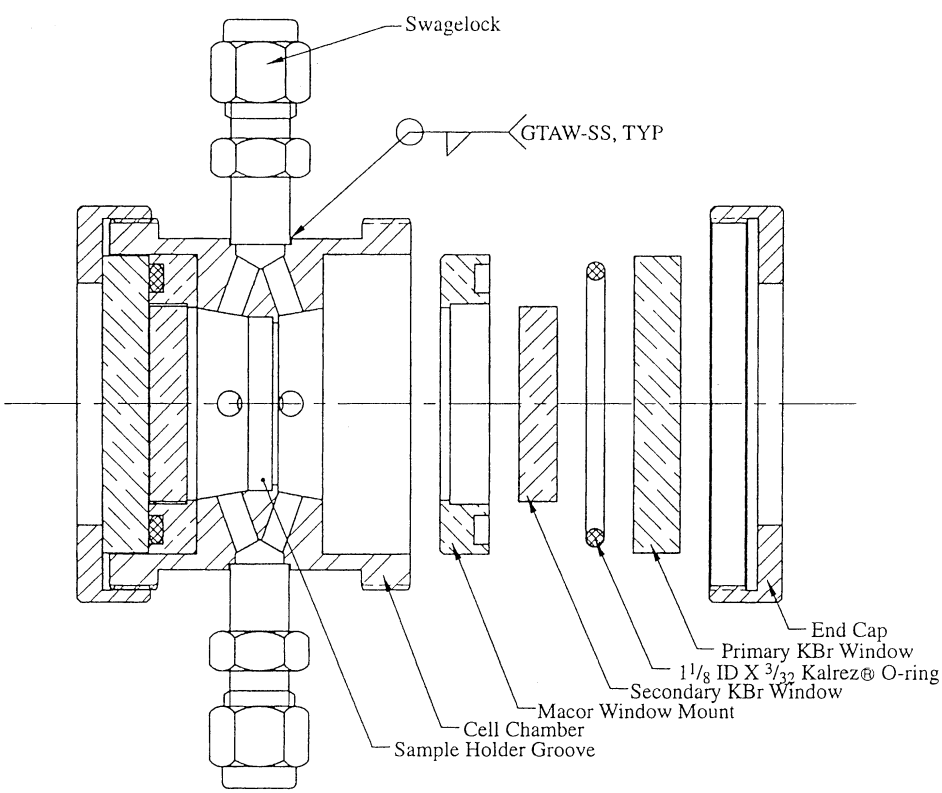

FIG. 1. Assembly view of the FTIR cell.

resistance heating wire (Omega Engineering) which was embedded in electric heater cement (Sauereisen). The cell could be heated to 400°C and evacuated to 10^{-2} Torr.

Gas and Liquid Delivery System

A gas delivery system was used to direct ultrapure N_2 carrier gas or a 10% oxygen–90% N_2 gas mixture into the cell. Research purity *n*-butane and 1,3-butadiene (Matheson) were used as hydrocarbon feeds. Moisture traps, oxygen traps, and CO_2 traps were present. Tylan mass flow controllers were used to regulate the flow. The system could deliver a continuous flow of $C_4H_n/O_2/N_2$, C_4H_n/N_2, O_2/N_2, or N_2; or, step changes between C_4H_n/N_2 and O_2/N_2 could be introduced. The flow rate of O_2/N_2 or pure N_2 was 50 ml/s for all studies. Liquid samples (20 μl) were introduced into the system by syringe injection into a Swagelok "T" installed on the gas line. Direct injection into the cell was also used. Solid samples were vaporized and introduced into the cell. All chemicals used in adsorption studies (except for *n*-butane and 1,3-butadiene) were purchased from Aldrich (purity typically above 95%).

Reaction and Adsorption Studies

Reaction and adsorption studies differed in the method of feeding the reactant. Prior to the transient studies, the FTIR cell was operated as a continuous flow microreactor. The concentration of *n*-butane and 1,3-butadiene was 5 mol% in N_2, and the concentration of oxygen was 10 mol% in N_2. Step changes consisting of C_4H_n/N_2 vs O_2/N_2 were performed using the above-mentioned gas delivery system. For the adsorption studies, compounds were injected into the system using a syringe. The behavior of adsorbates in the presence of N_2 or O_2/N_2 was then observed. For a gas flow rate of 50 ml/s, the residence time in the empty cell was less than 1 min.

RESULTS

A large number of spectra have been collected in our current studies, and the results were reproducible; only representative spectra have been presented in this paper. Unless otherwise indicated, the spectra displayed in each figure have the same intensity scale. Before analyzing the results of these studies, some general observations about the interpretation of the spectra can be made.

For FTIR studies using $(VO)_2P_2O_7$, only bands above 1300 cm^{-1} are observable due to strong adsorption by the catalyst in the region below 1300 cm^{-1}. In previous studies, bands present in the region of 2000–1300 cm^{-1} have been examined most extensively. Bands near 1850 and 1775 cm^{-1} are characteristic of the symmetric and asymmetric stretching vibrational modes of carbonyl groups for cyclic dicarbonyl compounds (22). The carbonyl groups of saturated aliphatic ketones (e.g., acetone, ethyl methyl ketone) have a stretching vibrational band at 1715 cm^{-1}. A variety of factors will cause the band position of carbonyl groups to shift (22, 23). For the studies reported here, the following guidelines can be used. A neighboring electron-withdrawing group or a strained ring will cause carbonyl stretching bands to be present at higher frequencies; a neighboring electron-donating group will make this band appear at lower frequencies. For example, the bands near 1715 cm^{-1} are typically due to the stretching vibration modes of carbonyl groups for saturated aliphatic ketones. A shift of the band from this position could result from interaction with the catalyst or could be due to formation of a strained ring. In regard to other surface species, alkenes may form π-complexes with the surface cations, and the band for $\nu_{C=C}$ may be at lower positions than typical gas-phase species (1670–1640 cm^{-1}). The magnitude of the shift can be in the range 10–100 cm^{-1} (24). Conjugation of unsaturated C=C bonds also lowers the position of this band. For example, $\nu_{C=C}$ for 2-butene is at 1660 cm^{-1} (25) while that for 1,3-butadiene is at 1587 cm^{-1} (26).

n-Butane

Reaction studies of *n*-butane involving step changes and continuous flow were performed at several temperatures from room temperature to 350°C. Figure 2 shows the

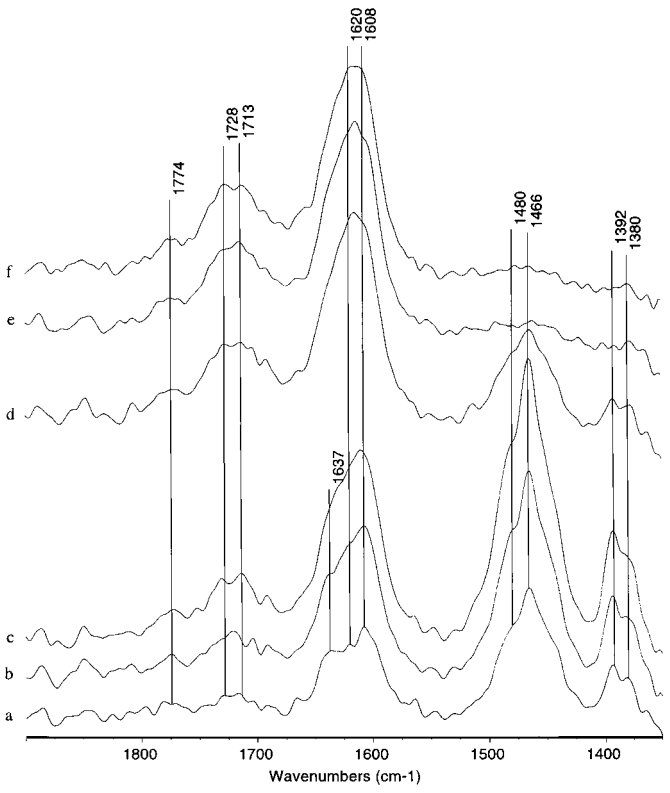

FIG. 2. *n*-Butane step change reaction at 50°C. Spectra a–c for the C_4H_{10}/N_2 step, d–f for the O_2/N_2 step. (a) 0 min, (b) 1 min, (c) 2 min, (d) 3 min, (e) 4 min, (f) 5 min.

spectra collected at 50°C under step change conditions (Figs. 2a–2c in C_4H_{10}/N_2; Figs. 2d–2f in O_2/N_2). Each step lasted about 3 min, and the time for each collection was less than 1 min. Strong bands near 1466 and 1392 cm^{-1} were due to gas-phase *n*-butane (asymmetrical and symmetrical CH_3 deformations, respectively). Bands near 1720 and 1620 cm^{-1} were prominent during the experiment. Bands at 1637, 1620, and 1608 cm^{-1} were apparent in Fig. 2a. The 1608 cm^{-1} band became more intense during the C_4H_{10}/N_2 step and obscured neighboring bands at 1637 and 1620 cm^{-1} (Figs. 2b, 2c). The maximum for these broad bands shifted to near 1615 cm^{-1} in the O_2/N_2 step (Figs. 2d–2f). These bands can be attributed to $\nu_{C=C}$ of adsorbed olefinic species. The difference in their positions may due to the presence of single C=C bonds (e.g., butene) or conjugated (e.g., 1,3-butadiene) C=C bonds. Adsorbed water also exhibits a band centered at about 1620 cm^{-1} (13), and water is a product of hydrocarbon oxidation. The bands around 1620 cm^{-1} can be partially attributed to adsorbed water. This assignment has also been supported by the observation of –OH vibrations near 3500 cm^{-1}. Broad bands in the region of 1750–1690 cm^{-1} (peaks approximately at 1728 and 1713 cm^{-1}) were also observed. These features were present in spectra obtained in the C_4H_{10}/N_2 step, but clearly became more intense in the O_2/N_2 step. Assignment of these bands to the carbonyl stretching vibration of noncyclic species is appropriate, as discussed previously. (As reported in the following discussion the adsorption of noncyclic carbonyl species such as ethyl methyl ketone, butyraldehyde, methyl vinyl ketone, and crotonaldehyde all resulted in major carbonyl stretching bands near 1720 cm^{-1}.)

Figure 3 provides spectra obtained at 200°C, with Figs. 3a–3c collected in the C_4H_{10}/N_2 step and Figs. 3d–3f collected in the O_2/N_2 step. Figures 3g–3l were obtained in a second similar C_4H_{10}/N_2–O_2/N_2 cycle. In the first C_4H_{10}/N_2 step (Figs. 3a–3c), bands at 1465 and 1396 cm^{-1} were due to gas-phase *n*-butane; the presence of gas-phase 1,3-butadiene was revealed by the doublets at 1830 and 1808 cm^{-1} and at 1605 and 1585 cm^{-1} (27). Bands around 1777, 1723, and in the region of 1680–1660 cm^{-1} were apparent after 2 min in the reaction (Figs. 3c–3l). In the first O_2/N_2 step (Figs. 3d–3f), bands due to gas-phase *n*-butane and 1,3-butadiene diminished, while the bands near 1777 cm^{-1} intensified significantly. In the second cycle (Figs. 3g–3l), bands at 1777, 1723, 1658, and 1598 cm^{-1} became more intense. In the O_2/N_2 step of the second cycle (Figs. 3j–3l), the band at 1854 cm^{-1} became evident. The associated bands at around 1854 and 1777 cm^{-1} indicate the generation of maleic anhydride.

The results of additional studies performed at 300°C are illustrated in Fig. 4, in which the catalyst was first treated with C_4H_{10}/N_2 for 1 min and then was exposed to O_2/N_2. The

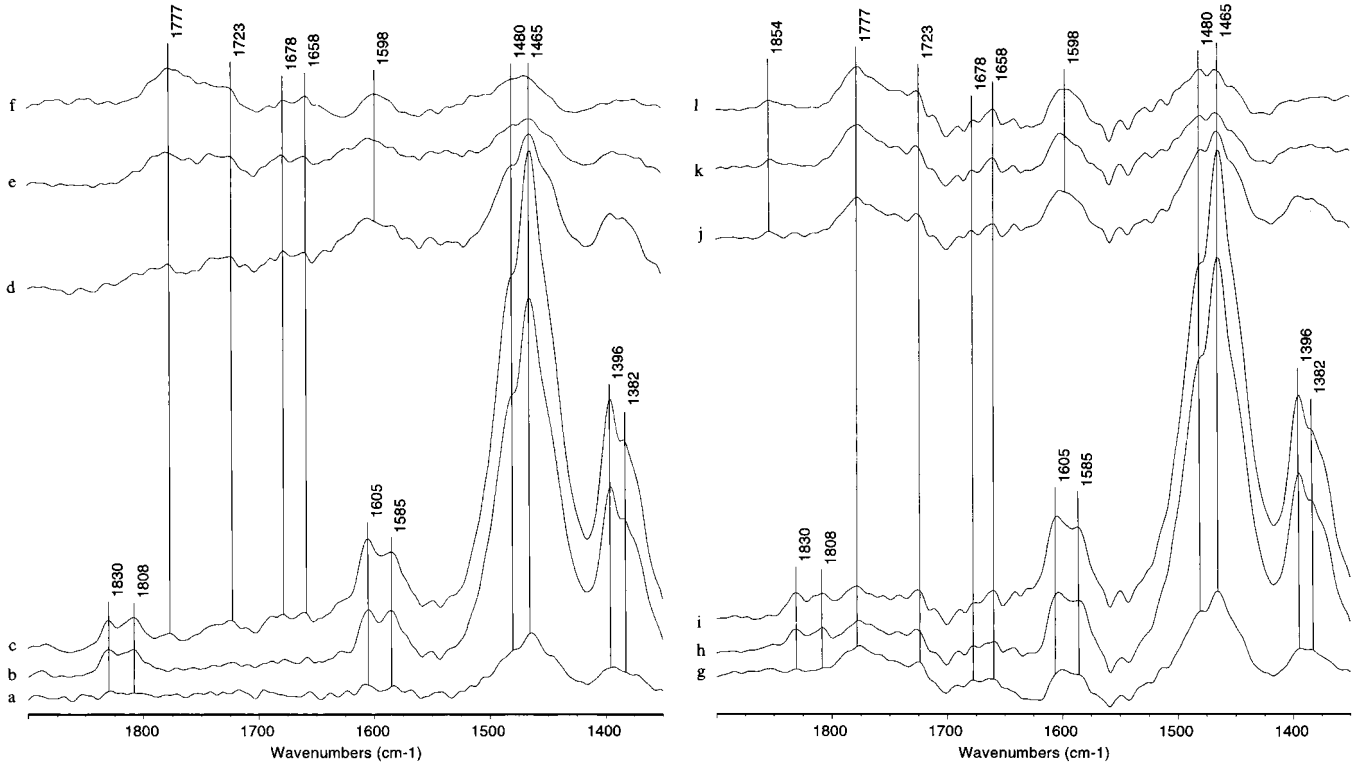

FIG. 3. *n*-Butane step change reaction at 200°C. (Left) First C_4H_{10}/N_2–O_2/N_2 cycle: spectra a–c for the C_4H_{10}/N_2 step, d–f for the O_2/N_2 step, g–i for the C_4H_{10}/N_2 step, and j–l for the O_2/N_2 step. (a) 0 min, (b) 1 min, (c) 2 min, (d) 3 min, (e) 4 min, (f) 5 min. (Right) Second C_4H_{10}/N_2–O_2/N_2 cycle: spectra g–i for the C_4H_{10}/N_2 step, and j–l for the O_2/N_2 step. (g) 6 min, (h) 7 min, (i) 8 min, (j) 9 min, (k) 10 min, (l) 11 min.

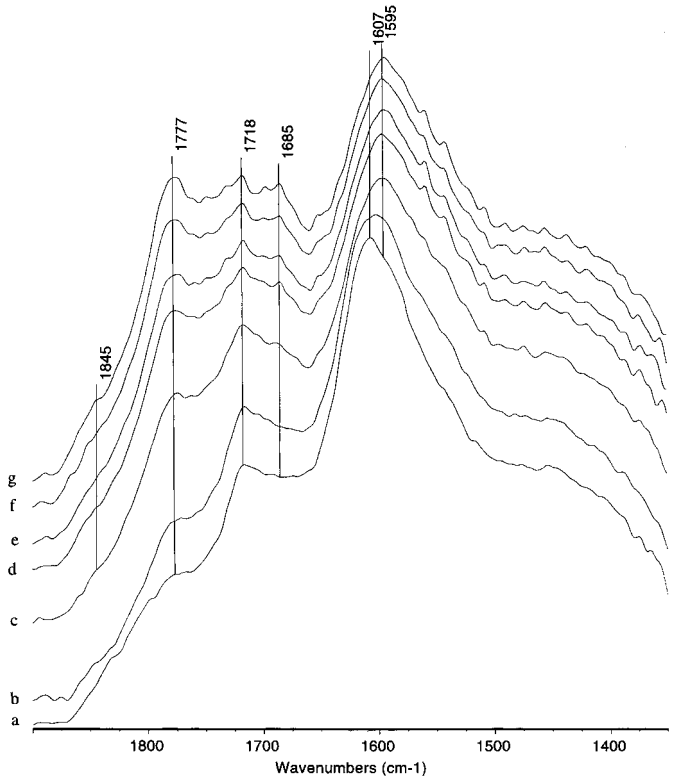

FIG. 4. Evolution of surface species in flowing O_2/N_2 after *n*-butane adsorption at 300°C. (a) 0 min, (b) 2 min, (c) 7 min, (d) 14 min, (e) 17 min, (f) 25 min, (g) 32 min.

spectra collected immediately after the adsorption (Fig. 4a) showed two major bands at around 1718 and 1607 cm^{-1} with a shoulder present at 1777 cm^{-1}. The relative intensity between the 1718 cm^{-1} band and the 1777 cm^{-1} band reversed as a function of time. A band at 1685 cm^{-1} became apparent after about 7 min (Fig. 4c); the 1777 cm^{-1} band and its shoulder band at 1845 cm^{-1} clearly were more intense in the last spectrum (Fig. 4g). The shift in the position of the 1607 cm^{-1} band to 1595 cm^{-1} may be explained by the presence of more maleic anhydride on the surface which has a $\nu_{C=C}$ in the region of 1600–1590 cm^{-1} (28).

Wenig and Schrader (10) reported spectra for steady state reaction of *n*-butane on VPO catalysts with P/V ratios of 0.9, 1.0, 1.1 at various temperatures. Bands near 1720 and 1620 cm^{-1} were observed in all studies. The 1720 cm^{-1} band was already present at 100 and 200°C, but bands indicating formation of maleic anhydride were not observed under these conditions. The 1720 cm^{-1} band was a major band in most of the spectra presented. FTIR spectra of *n*-butane and 1-butene adsorption on $(VO)_2P_2O_7$ reported by Busca and Centi (18) were similar. Bands at 1720–1710 cm^{-1} and 1620 cm^{-1} were observed upon hydrocarbon adsorption. Bands characteristic of maleic anhydride at 1850 and 1780 cm^{-1} were detected and became more intense after oxygen was introduced at higher temperatures.

1,3-Butadiene

Figure 5 shows the spectra collected at 100°C during 1,3-butadiene step-change reaction studies. Doublets at 1829 and 1810 cm^{-1} and at 1605 and 1587 cm^{-1} were due to gas-phase 1,3-butadiene. The broad shoulder band in the region 1390–1370 cm^{-1} was also partially attributed to gas-phase 1,3-butadiene which has a doublet at 1390 and 1371 cm^{-1} (in-plane bending vibration of terminal vinyl group $\delta_{=CH_2}$). A broad band with three maxima at 1550, 1487, and 1466 cm^{-1} could be observed. The relative intensity between the 1487 and 1466 cm^{-1} bands changed as the reaction proceeded. This phenomenon was persistent in studies at temperatures of 250°C and below. The band at 1550 cm^{-1} may be ascribed to the asymmetric double bond stretching mode of furan (ν_{14}). The band at 1487 cm^{-1} was due to the ring "breathing" mode (ν_3) of furan, and the 1466 cm^{-1} band was attributed to a combination tone of ring bending modes of furan ($\nu_9 + \nu_{21}$) (29, 30). It should be noticed that *n*-butane adsorption also exhibited bands at 1466 and 1392 cm^{-1} (Fig. 2), but they were due to methyl deformation modes of *n*-butane. At 100°C, adsorption of 1,3-butadiene did not result in the formation of maleic anhydride.

Figure 6 shows the spectra collected at 300°C during step change reaction studies. Figures 6a–6f were collected in the first C_4H_6/N_2–O_2/N_2 cycle (Figs. 6a–6c in the C_4H_6/N_2 step

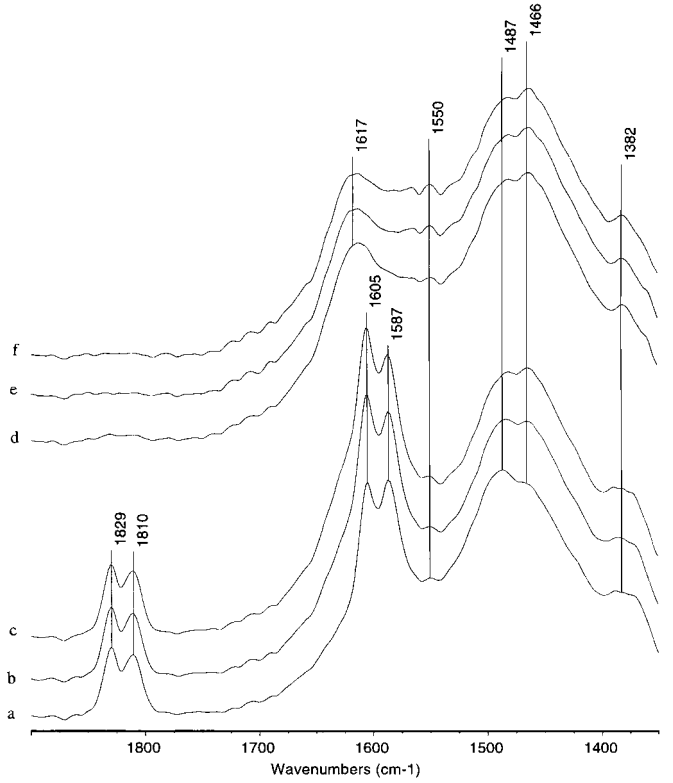

FIG. 5. 1,3-Butadiene step change reaction at 100°C. Spectra a–c for the C_4H_6/N_2 step, d–f for the O_2/N_2 step. (a) 0 min, (b) 1 min, (c) 2 min, (d) 3 min, (e) 4 min, (f) min.

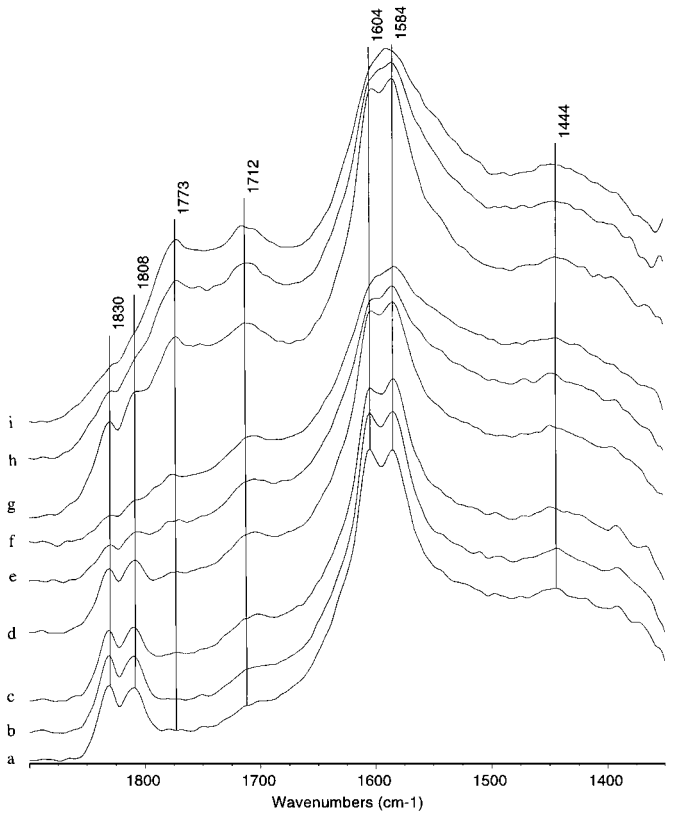

FIG. 6. 1,3-Butadiene step change reaction at 300°C. Spectra a–f were collected for the first C_4H_6/N_2–O_2/N_2 cycle: a–c for the C_4H_6/N_2 step, d–f for the O_2/N_2 step. Spectra g–i were collected for the O_2/N_2 step of the third C_4H_6/N_2–O_2/N_2 cycle. (a) 0 min, (b) 1 min, (c) 2 min, (d) 3 min, (e) 4 min, (f) 5 min, (g) 15 min, (h) 16 min, (i) 17 min.

and Figs. 6d–6f in the O_2/N_2 step). Figures 6g–6i were collected in the O_2/N_2 step of the third C_4H_6/N_2–O_2/N_2 cycle. Bands at 1830, 1808, 1604, and 1584 cm^{-1} were again due to gas-phase 1,3-butadiene; a shoulder band at 1720–1700 cm^{-1} intensified quickly in the first C_4H_6/N_2 step (Figs. 6a–6c). The band near 1773 cm^{-1} was detectable in the following O_2/N_2 step (Figs. 6d–6f). After three C_4H_6/N_2–O_2/N_2 cycles, the bands near 1773 and 1712 cm^{-1} were clearly prominent (Figs. 6g–6i).

1,3-Butadiene oxidation on VPO catalysts of different P/V ratios at 300°C was reported by Wenig and Schrader (11). An intense band with two maxima at 1720 and 1690 cm^{-1}, which was apparently due to carbonyl stretching vibrations of noncyclic species, was observed to coexist with bands attributed to maleic anhydride. Ramstetter and Baerns (16) reported a band in this region at 1680 cm^{-1}. For 1,3-butadiene adsorption and oxidation on V_2O_5–TiO_2 studied by Busca *et al.* (19), the following spectral features were observed: bands at 1490 and 1455 cm^{-1} (attributed to molecular furan), a strong band at 1560 cm^{-1} (assigned to perturbed furan), a band at 1720 cm^{-1} ($\nu_{C=O}$), bands at 1870 and 1790 cm^{-1} (assigned to maleic anhydride), and bands at 1540 and 1440 cm^{-1} (attributed to carboxylate ions). Aside from bands due to carboxylate ions, the band positions which were detected were at similar positions to those for our current study.

2,5-Dihydrofuran and 2,3-Dihydrofuran

Spectra for the adsorption of 2,5-dihydrofuran at 100°C are shown in Fig. 7. According to Klots and Collier (31), liquid-phase 2,5-dihydrofuran exhibits bands at 1777 (vw), 1694 (vw), 1618 (w), 1587 (w), 1483 (w), and 1345 cm^{-1} (m); liquid-phase 2,3-dihydrofuran has bands at 1837 (w), 1766 (w), 1735 (w), 1619 (s), 1590 (sh), 1453 (w), and 1375 (mw). Most of the spectral features in Fig. 7a—the bands at 1844, 1776, 1739, 1621, 1580, 1479, and 1350 cm^{-1}—were attributed to 2,3-dihydrofuran. The band at 1726 cm^{-1}, which increased while other bands due to the dihydrofurans decreased, was characteristic of a noncyclic carbonyl species. This indicated that dihydrofuran experienced ring cleavage to form carbonyl species after adsorption.

The adsorption of 2,5-dihydrofuran at 300°C rapidly generated bands near 1785 and 1617 cm^{-1} with two shoulder bands around 1705 and 1487 cm^{-1} (Fig. 8). As observed in *n*-butane and 1,3-butadiene adsorption studies at 300°C, the 1784 cm^{-1} band became more intense as the reaction continued while other bands diminished in intensity. The band

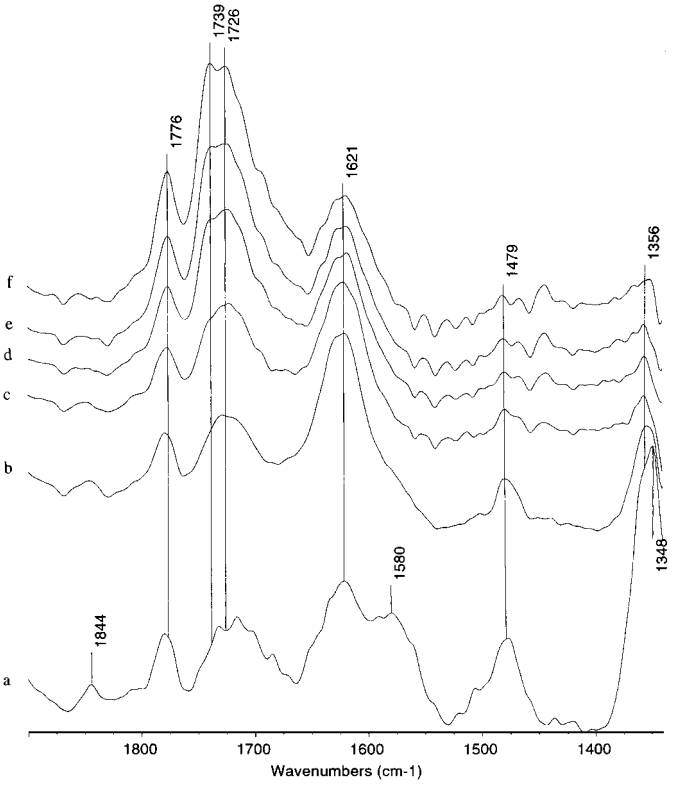

FIG. 7. Evolution of surface species in flowing O_2/N_2 after 2,5-dihydrofuran adsorption at 100°C. (a) 0 min, (b) 1 min, (c) 3 min, (d) 5 min, (e) 7 min, (f) 10 min.

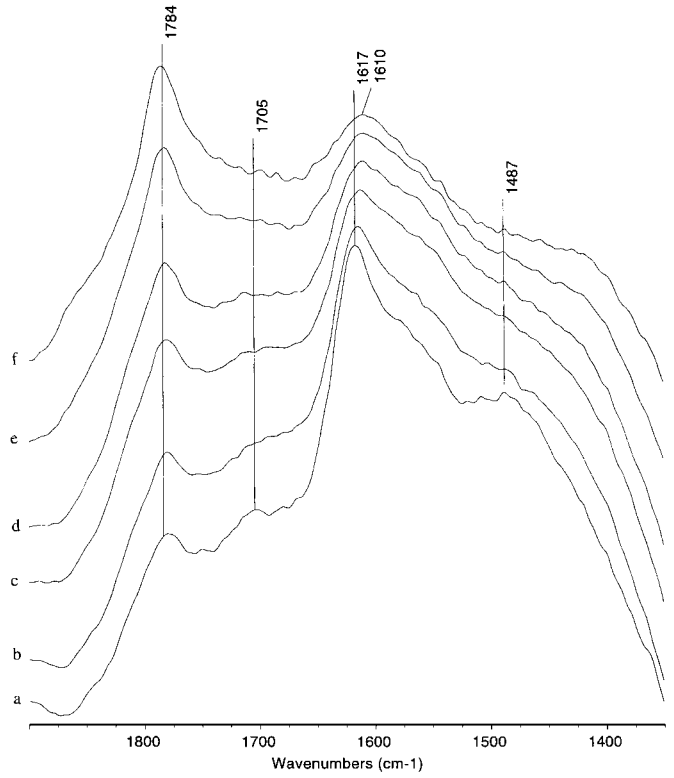

FIG. 8. Evolution of surface species in flowing O_2/N_2 after 2,5-dihydrofuran adsorption at 300°C. (a) 0 min, (b) 2 min, (c) 4 min, (d) 7 min, (e) 20 min, (f) 55 min.

near 1705 cm^{-1} was more apparent in the first spectrum and became obscured as the 1784 cm^{-1} band became more prominent. The spectra of 2,5-dihydrofuran on $(VO)_2P_2O_7$ presented by Busca and Centi (18) also exhibited a band at 1715 cm^{-1} together with bands at 1840, 1780, and 1620 cm^{-1}.

The adsorption of 2,3-dihydrofuran at 150°C also resulted in the formation of the band at 1725 cm^{-1} which increased in intensity with time (Figs. 9a–9d). Bands at 1772, 1617, 1453, and 1357 cm^{-1} in the early spectra were due to molecular 2,3-dihydrofuran. These bands decreased in intensity compared to the bands near 1725 and 1695 cm^{-1} which were indicative of noncyclic species formed by ring cleavage. After the sample was held at 150°C for 30 min, the reaction temperature was slowly raised to 300°C over 1 h [the generation of water resulted in increased "noise" in the region of 1650–1400 cm^{-1} (Figs. 9e–9h)]. At higher temperatures, bands due to maleic anhydride (1843 and 1778 cm^{-1}) emerged and became more intense. The apparent shift of the 1725 cm^{-1} band into the region 1740–1730 cm^{-1} may be partially attributable to the formation of maleic anhydride which has a shoulder band near 1750 cm^{-1}.

Furan

The adsorption of furan at 100°C on vanadyl pyrophosphate is shown in Fig. 10. The bottom spectrum was collected directly after injection of vapor phase furan. The strong band at 1484 cm^{-1} was due to the furan ring "breathing" mode (ν_3), and the band near 1577 cm^{-1} was assigned to the combination of the bending vibrations for furan ring ($\nu_{19} + \nu_{20}$) (29). The weak bands at 1871, 1851, and 1774 cm^{-1} could also be associated with molecular adsorption of furan. The broad band centered at 1714 cm^{-1} in the bottom spectrum (Fig. 10a) was ascribed to overtone and combination bands of the bending vibrations of the ring and C–H bonds (29, 30). Upon exposure to O_2/N_2, bands due to gas-phase furan at 1577 and 1484 cm^{-1} disappeared quickly; weak bands around 1559, 1494, and 1458 cm^{-1} in the later spectrum were due to surface-bound furan species. However, the broad band around 1717 cm^{-1} persisted and became the major feature. This band was not attributable to molecular furan since it should have decreased in intensity together with the 1577 and 1484 cm^{-1} bands. Assignment to a noncyclic carbonyl species was more appropriate.

The adsorption of furan at 300°C resulted in bands at around 1786, 1723, 1550, 1488, and 1453 cm^{-1} (Fig. 11). The 1550, 1488, and 1453 cm^{-1} bands were due to surface-bound furan molecules. After 3 h, the 1858 cm^{-1} band was more distinct, the 1786 cm^{-1} band was stronger, and the bands

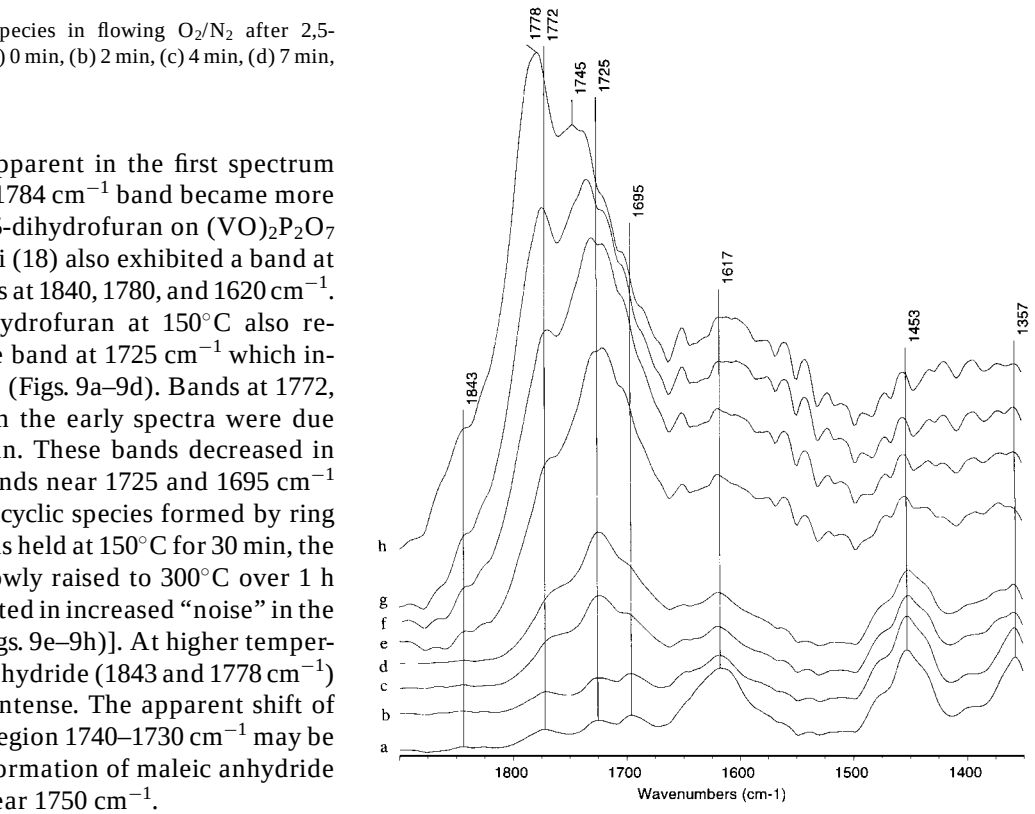

FIG. 9. Evolution of surface species in flowing O_2/N_2 after 2,3-dihydrofuran adsorption: a–d collected at 150°C, e–h collected during and after the temperature was raised to 300°C. (a) 0 min, (b) 1 min, (c) 9 min, (d) 33 min, (e) 48 min, (f) 72 min, (g) 90 min, (h) 105 min.

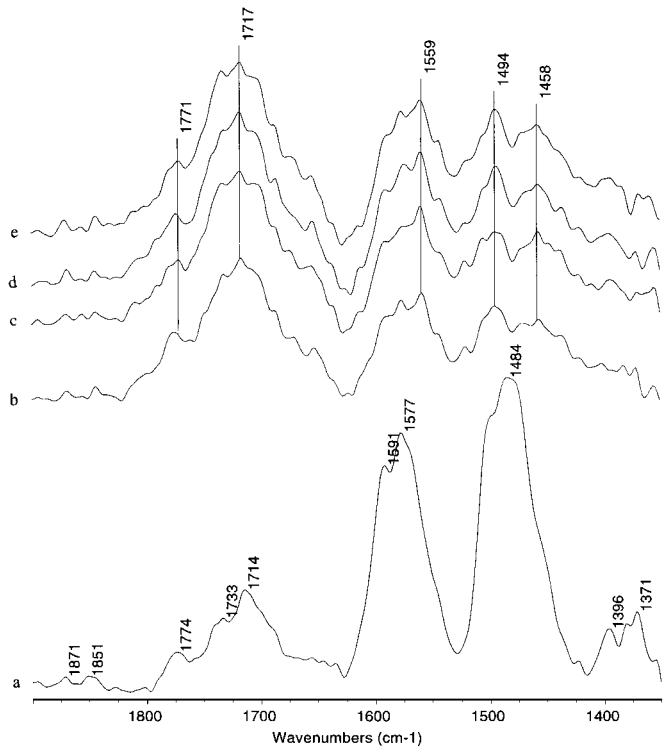

FIG. 10. Evolution of surface species in flowing O_2/N_2 after furan adsorption at 100°C. (a) 0 min, (b) 1 min, (c) 3 min, (d) 7 min, (e) 10 min.

due to furan (1550, 1488, and 1453 cm^{-1}) decreased. Two new maxima at 1611 and 1428 cm^{-1} were formed which may be due to adsorbed species with C=C double bonds and carboxylate species, respectively.

Ramstetter and Baerns (16) studied the adsorption of furan on an alumina-supported VPO catalyst. Because of changes in the relative intensities of the 1490 and 1455 cm^{-1} bands, an addition complex of the furan ring at the α-position to the catalyst was believed to exist on the catalyst surface. A broad band in the region of 1600–1550 cm^{-1} was also prominent. More importantly, a band at 1690 cm^{-1} was formed upon adsorption which was likely due to a carbonyl species. In another study performed by Do and Baerns (17), the 1690 cm^{-1} band was also observed and was assigned to an α,β-unsaturated aldehyde.

2(5H)-Furanone

Spectra for the adsorption of 2(5*H*)-furanone at 100°C are shown in Fig. 12. The split carbonyl stretching bands at 1777 and 1741 cm^{-1} are observed typically for unsaturated five-membered ring lactones in which the double bond is conjugated with the carbonyl group (32). The treatment in O_2/N_2 at 100°C eventually resulted in the disappearance of these two bands. A broad band in the region of 1740–1690 cm^{-1} was evident which was characteristic of noncyclic carbonyl compounds.

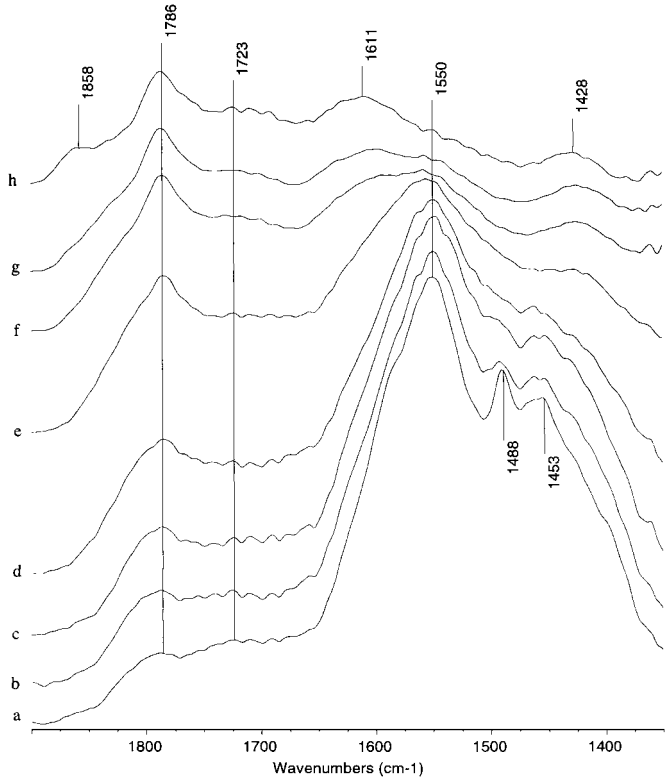

FIG. 11. Evolution of surface species in flowing O_2/N_2 after furan adsorption at 300°C. (a) 0 min, (b) 2 min, (c) 5 min, (d) 23 min, (e) 36 min, (f) 60 min, (g) 104 min, (h) 180 min.

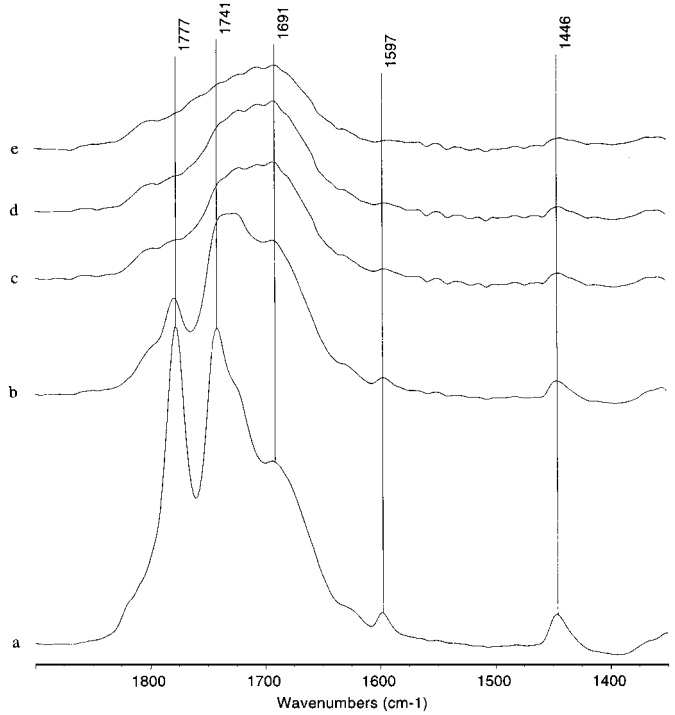

FIG. 12. Evolution of surface species in flowing O_2/N_2 after 2(5*H*)-furanone adsorption at 100°C. (a) 0 min, (b) 5 min, (c) 30 min, (d) 55 min, (e) 105 min.

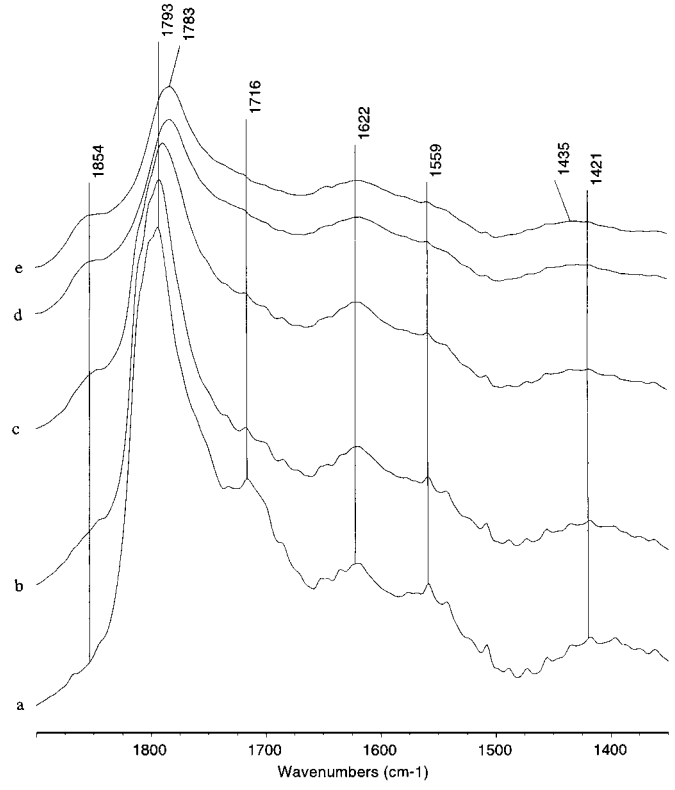

FIG. 13. Evolution of surface species in flowing O_2/N_2 after 2(5*H*)-furanone adsorption at 300°C. (a) 0 min, (b) 3 min, (c) 11 min, (d) 44 min, (e) 67 min.

The adsorption of 2(5*H*)-furanone at 300°C instantly generated an intense peak at 1793 cm^{-1} with a shoulder band near 1716 cm^{-1} (Fig. 13). Maxima near 1622 ($\nu_{C=C}$), 1559 (ν_{as,COO^-}), and 1421 cm^{-1} (ν_{as,COO^-}) were also observed. At longer time periods, the intensity of the 1793 cm^{-1} peak decreased while the intensities of the 1783 cm^{-1} band and its 1850 cm^{-1} shoulder band increased. Formation of maleic anhydride was indicated.

Ramstetter and Baerns (16) also studied 2(5*H*)-furanone adsorption on a supported VPO catalyst. Other than bands due to molecular and surface-bound 2(5*H*)-furanone, a broad band (maxima at 1705 and 1690 cm^{-1}) was detected at 100°C which was assigned to aldehyde species.

γ-Butyrolactone

Figure 14 shows the evolution of spectra following the adsorption of γ-butyrolactone. The bands at 1813 and 1749 cm^{-1} were due to the carbonyl stretching mode of γ-butyrolactone. The band at 1699 cm^{-1} was attributed to the formation of a noncyclic carbonyl species. The band in the region of 1640–1620 cm^{-1} was likely due to generation of C=C bonds or water. Bands due to molecular γ-butyrolactone decreased with time while the noncyclic carbonyl stretching band (~1699 cm^{-1}) became dominant in the later spectra. There was no evidence for the formation of maleic anhydride (bands at 1850 and 1780 cm^{-1}).

5-Hydroxy-2(5H)-Furanone

The result of 5-hydroxy-2(5*H*)-furanone adsorption at 200°C is shown in Fig. 15. Three major bands were observed at 1800, 1756, and 1707 cm^{-1} with a shoulder band at 1729 cm^{-1}: all of these bands are in the carbonyl stretching vibration region. The first two bands are likely due to carbonyl stretching modes of 5-hydroxy-2(5*H*)-furanone. The bands near 1729 and 1707 cm^{-1} were due to the noncyclic carbonyl compounds generated in the reaction. The 1800 and 1756 cm^{-1} bands diminished quickly, and the band at 1707 cm^{-1} was very intense in the beginning but slowly became less apparent. Similar behavior was observed for the bands at around 1564 and 1405 cm^{-1} which were attributed to carboxylate species. For adsorption studies at 100–250°C, prolonged adsorption of 5-hydroxy-2(5*H*)-furanone did not produce a detectable amount of maleic anhydride.

Maleic Anhydride

The adsorption of maleic anhydride on the catalyst at 100°C is shown in Fig. 16. The bands near 1851, 1795–1773, and a shoulder band at 1754 cm^{-1} were due to maleic anhydride (28). The bands at around 1683 (shoulder), 1565, and 1451 cm^{-1} were the result of transformation of the adsorbed

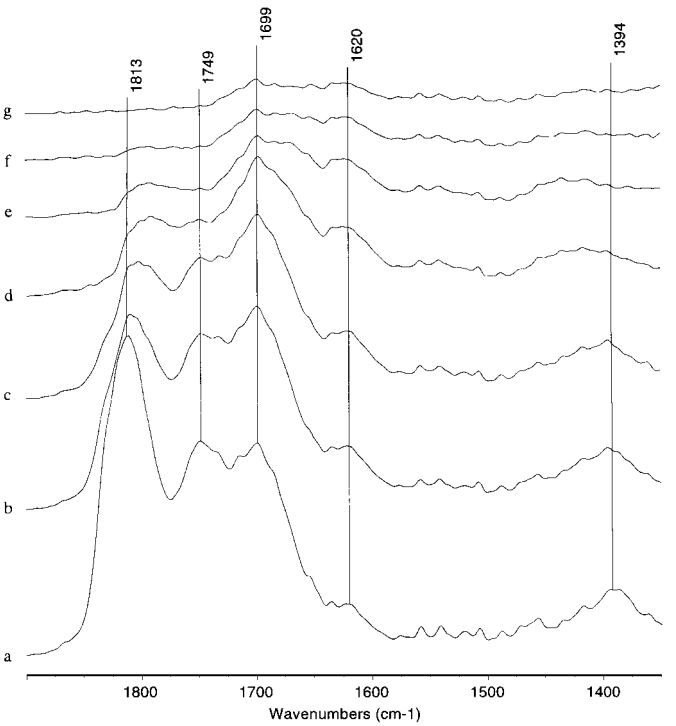

FIG. 14. Evolution of surface species in flowing O_2/N_2 after γ-butyrolactone adsorption at 300°C. (a) 0 min, (b) 3 min, (c) 5 min, (d) 9 min, (e) 16 min, (f) 21 min, (g) 28 min.

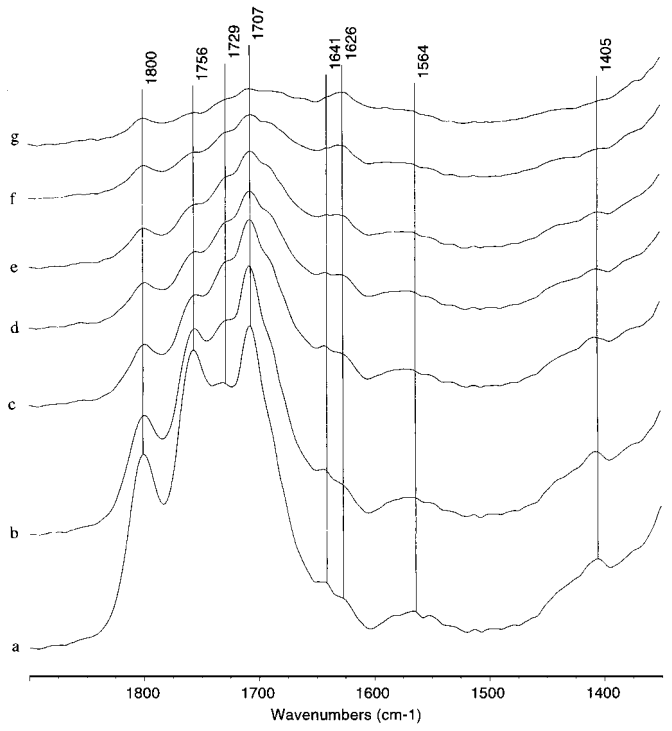

FIG. 15. Evolution of surface species in flowing O_2/N_2 after 5-hydroxy-2(5*H*)-furanone adsorption at 200°C. (a) 0 min, (b) 2 min, (c) 5 min, (d) 10 min, (e) 13 min, (f) 20 min, (g) 34 min.

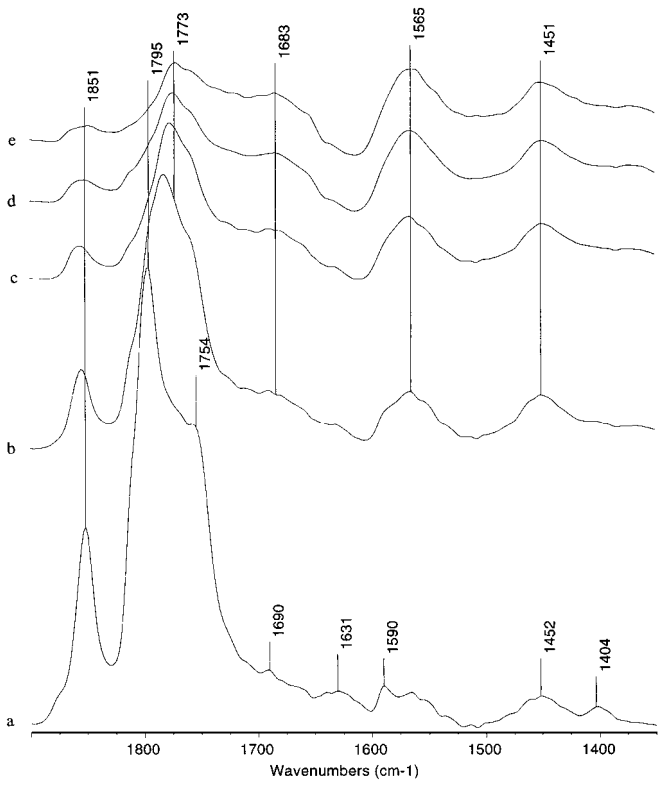

FIG. 16. Evolution of surface species in flowing O_2/N_2 after maleic anhydride adsorption at 100°C. (a) 0 min, (b) 2 min, (c) 6 min, (d) 13 min, (e) 19 min.

species. The shoulder band near 1683 cm^{-1} was more discernable in the later spectra when the 1780 cm^{-1} band had substantially decreased in intensity. The 1683 cm^{-1} band was likely due to a surface-bound aldehyde complex. The 1565 and 1451 cm^{-1} bands corresponded to the asymmetric and symmetric vibration of carboxylate ions (33). At higher temperatures (e.g., 200°C), the decomposition of maleic anhydride was more rapid.

Adsorption studies of maleic anhydride by Puttock *et al.* (15) and Wenig *et al.* (12) provided little information due to the interference from the strong adsorption bands of the VPO catalyst. However, bands due to maleic anhydride and carboxylate ions could be detected. In the studies by Baerns *et al.* (16, 17), the 1720 cm^{-1} band and a shoulder at 1680 cm^{-1} were observed.

Ethyl Methyl Ketone and Butyraldehyde (C_4H_8O)

The adsorption of ethyl methyl ketone at 300°C (Fig. 17) resulted in the rapid observation of a carbonyl stretching band at 1724 cm^{-1}, a C=C stretching band at 1620 cm^{-1}, and a band in the region of 1790–1770 cm^{-1} (characteristic of maleic anhydride). As reaction continued, the bands near 1780 and 1850 cm^{-1} were became dominant while the 1724 and 1620 cm^{-1} bands decreased accordingly. The band around 1427 cm^{-1} indicated the generation of carboxylate species.

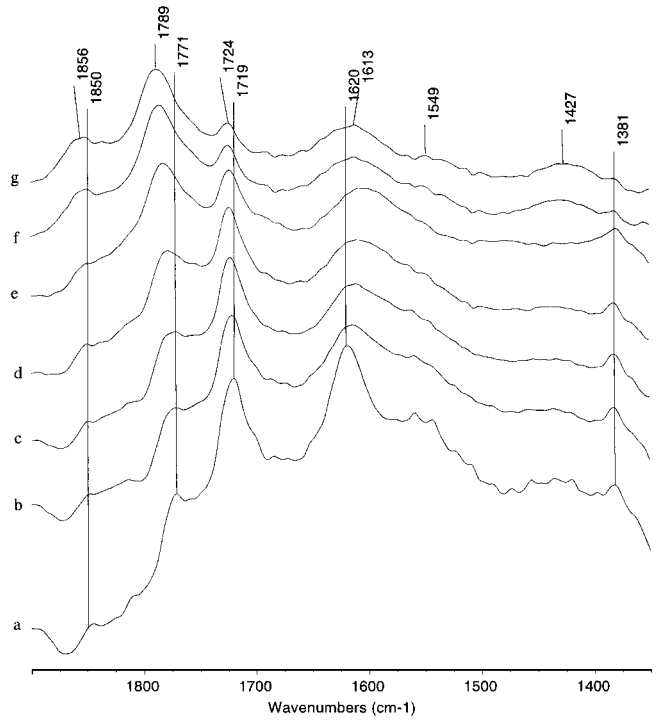

FIG. 17. Evolution of surface species in flowing O_2/N_2 after ethyl methyl ketone adsorption at 300°C. (a) 0 min, (b) 2 min, (c) 7 min, (d) 19 min, (e) 39 min, (f) 99 min, (g) 154 min.

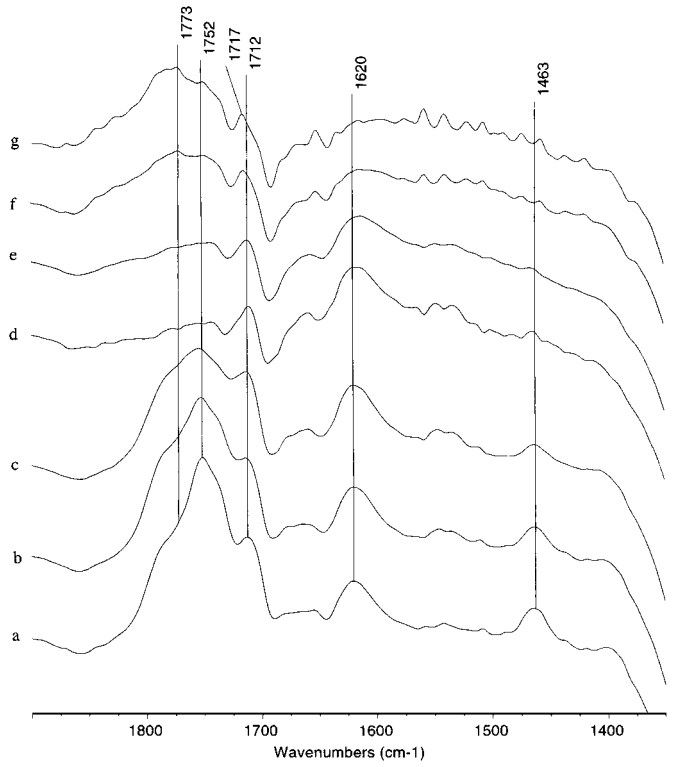

FIG. 18. Evolution of surface species in flowing O_2/N_2 butyraldehyde adsorption at 300°C. (a) 0 min, (b) 2 min, (c) 6 min, (d) 8 min, (e) 18 min, (f) 33 min, (g) 44 min.

Figure 18 provides spectra for butyraldehyde adsorption on the catalyst at 300°C. The 1752 cm^{-1} band originated from butyraldehyde whose carbonyl-stretching band was at a higher position than ketones (22, 23). The band at around 1620 cm^{-1} was ascribed to the C=C stretching mode. The band near 1712 cm^{-1} likely resulted form a carbonyl group conjugated with the C=C bond. In the earlier spectra, the 1752 cm^{-1} band decreased while the 1712 cm^{-1} band grew which indicated the formation of an unsaturated carbonyl compound. Later in the reaction, the growth of the maximum at 1773 cm^{-1} indicated the formation maleic anhydride.

Ethyl methyl ketone and butyraldehyde are saturated compounds. In both cases spectral features due to the C=C double bonds were generated quickly as indicated by the emergence of the characteristic band at 1620 cm^{-1}. As the reaction proceeded, this band decreased in intensity with the carbonyl stretching band (~1720 cm^{-1}). This indicated that hydrogen abstraction occurred upon adsorption to form an unsaturated noncyclic species which was then converted to maleic anhydride.

Methyl Vinyl Ketone and Crotonaldehyde (C_4H_6O)

The nature of methyl vinyl ketone adsorption was observed to be nearly identical to that of ethyl methyl ketone: the intensity of bands near 1711 cm^{-1} ($\nu_{C=O}$ of noncyclic species) and 1618 cm^{-1} ($\nu_{C=C}$) decreased while the intensity of the 1778 cm^{-1} band increased. A shoulder band at 1853 cm^{-1} behaved similarly (Fig. 19).

FTIR spectra for crotonaldehyde adsorption are shown in Fig. 20. The doublet at 1722 and 1707 cm^{-1} was due to gas-phase crotonaldehyde. A shoulder band at 1674 cm^{-1} was also present in the region for carbonyl stretching modes. The adsorption again exhibited similar results in which maleic anhydride (indicated by the band around 1779 cm^{-1}) was produced while the intensities of bands for open chain carbonyl compound (~1701 cm^{-1}) and C=C bonds (~1620 cm^{-1}) diminished.

Methyl Acrylate, Vinyl Acetate, Vinyl Acetic Acid, Crotonic Acid ($C_4H_6O_2$)

Each of these compounds contains two oxygen atoms, one of which is incorporated in a carbonyl group. An intense band near 1720 cm^{-1} was observed in all cases when these compounds were adsorbed on the catalyst surface. However, adsorption at the same conditions involved in the previous studies did not produce detectable amounts of maleic anhydride.

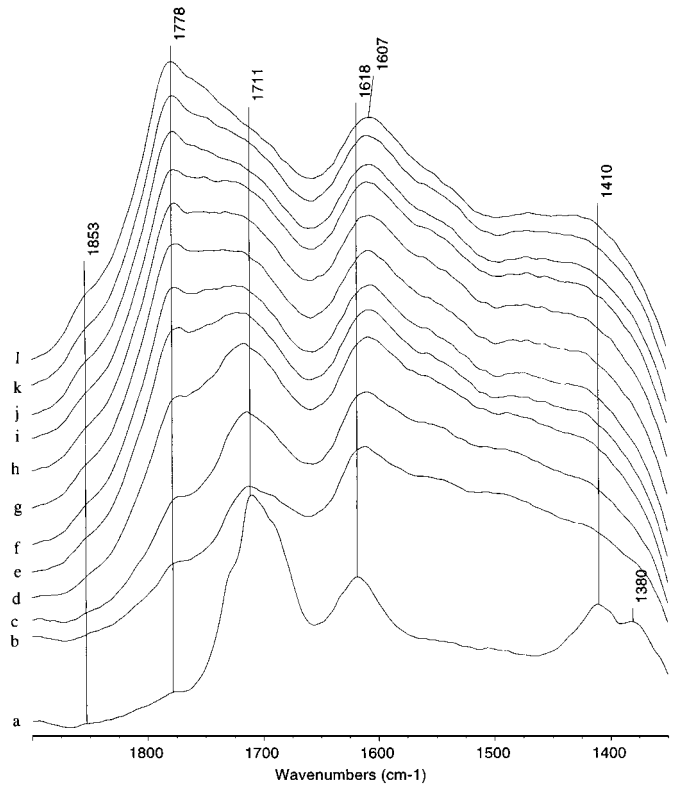

FIG. 19. Evolution of surface species in flowing O_2/N_2 after methyl vinyl ketone adsorption at 300°C. (a) 0 min, (b) 2 min, (c) 6 min, (d) 19 min, (e) 32 min, (f) 39 min, (g) 43 min, (h) 48 min, (i) 56 min, (j) 62 min, (k) 76 min, (l) 90 min.

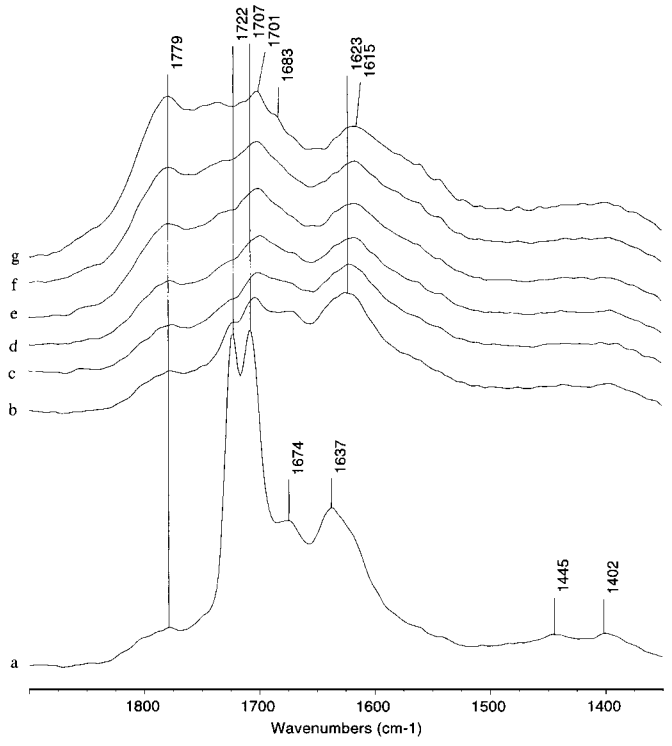

FIG. 20. Evolution of surface species in flowing O_2/N_2 after crotonaldehyde adsorption at 300°C. (a) 0 min, (b) 3 min, (c) 4 min, (d) 8 min, (e) 12 min, (f) 25 min, (g) 47 min.

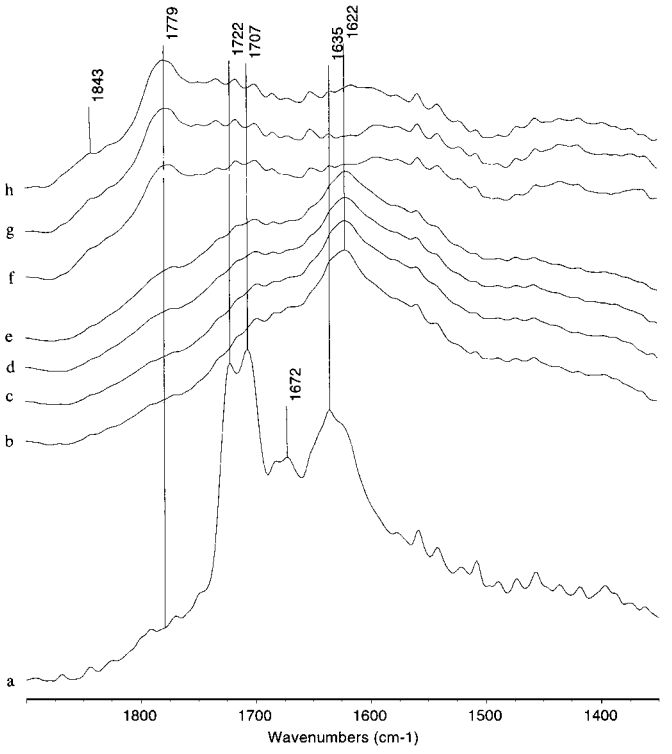

FIG. 21. Evolution of surface species in flowing O_2/N_2 after 2-butene-1,4-diol adsorption at 300°C. (a) 0 min, (b) 2 min, (c) 4 min, (d) 8 min, (e) 14 min, (f) 34 min, (g) 49 min, (h) 90 min.

2-Butene-1,4-diol ($C_4H_8O_2$)

Although 2-butene-1,4-diol showed no signs of reaction at 150°C in the empty cell, this compound reacted at 300°C in the gas-phase to produce crotonaldehyde. Adsorption of 2-butene-1,4-diol on the VPO catalyst (Fig. 21) also exhibited behavior the same as that for crotonaldehyde adsorption (Fig. 20).

Maleic Acid and Fumaric Acid ($C_4H_4O_4$)

Maleic acid can be readily dehydrated to maleic anhydride upon heating in the gas-phase. The adsorption of maleic acid on the catalyst at 150°C is shown in Fig. 22. Bands near 1850, 1775, 1722, 1682, 1635, 1567, and 1409 cm^{-1} were detected. The two carbonyl bands at 1850 and 1775 cm^{-1} (maleic anhydride) were the result of gas-phase dehydration. The adsorbed species showed split carbonyl stretching bands at 1722 and 1682 cm^{-1}. The bands at 1567 and 1409 cm^{-1} were due to carboxylate species. The adsorption pattern resembles the results for maleic anhydride adsorption (Fig. 16). At 250°C, surface species decomposed to carbon oxides very quickly.

Fumaric acid adsorption on the catalyst at 200°C (Fig. 23) exhibited a pattern similar to that for maleic acid adsorption: a carbonyl stretching band at 1720 cm^{-1}, a C=C double bond stretching band at 1643 cm^{-1}, and carboxylate ion

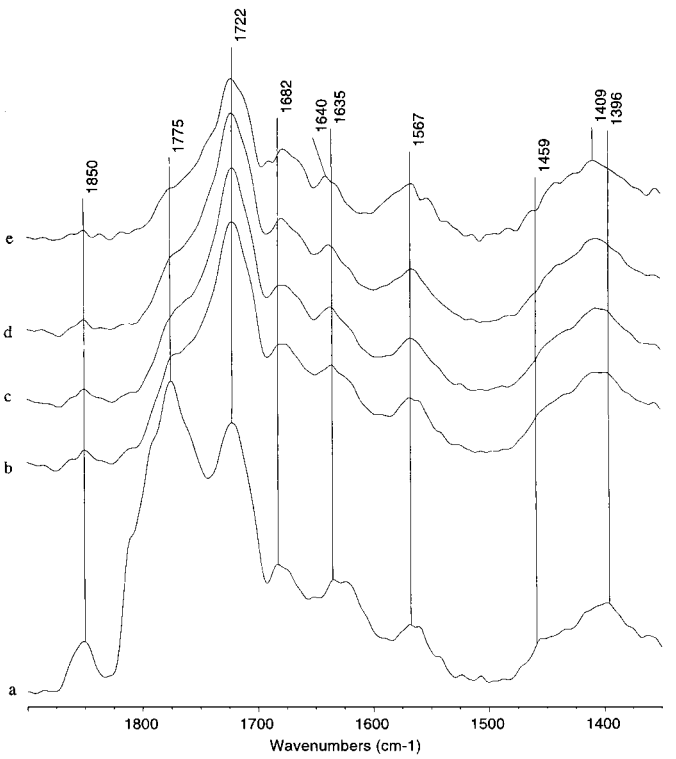

FIG. 22. Evolution of surface species in flowing N_2 after maleic acid adsorption at 150°C. (a) 0 min, (b) 1 min, (c) 3 min, (d) 6 min, (e) 25 min.

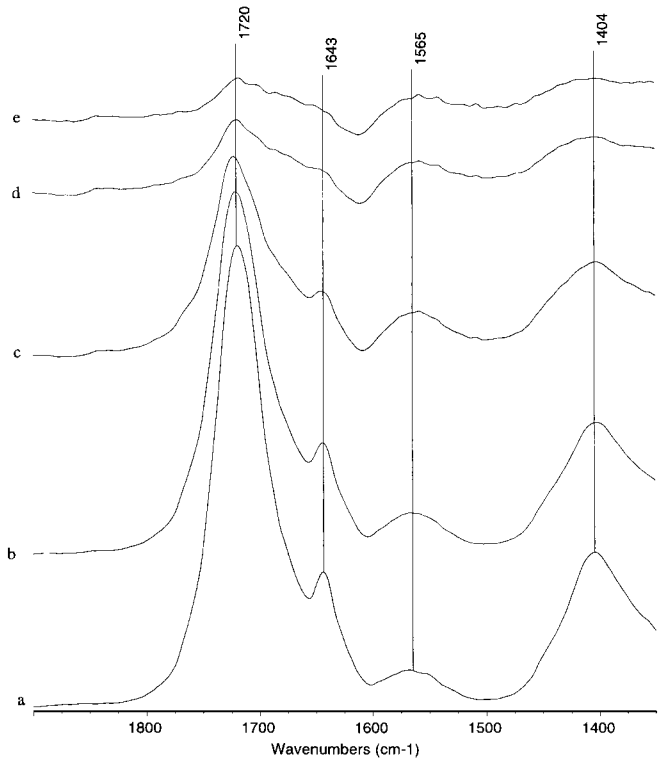

FIG. 23. Evolution of surface species in flowing N_2 after fumaric acid adsorption at 200°C. (a) 0 min, (b) 7 min, (c) 15 min, (d) 20 min, (e) 25 min.

bands at 1565 and 1404 cm^{-1} were observed. The surface species also decomposed quickly at higher temperatures ($T > 250$°C). The gas-phase dehydration of fumaric acid to maleic anhydride can occur at 300°C.

The shifts in carbonyl stretching bands were interesting: adsorbed maleic acid exhibited shifts in band positions [bands at 1720 and 1680 cm^{-1} compared to its typical position at 1705 cm^{-1} (33)]. The carbonyl band of furamic acid shifted from its normal position at 1680 to 1720 cm^{-1}, and spectra did not show a distinguishable band at 1680 cm^{-1} at temperatures where maleic anhydride was not produced (150–250°C). Maleic and fumaric acid are rotational isomers. At higher temperatures, their adsorbed forms should form an identical surface complex. Therefore, the band at 1682 cm^{-1} in Fig. 22 was likely a result of chemical conversion of maleic acid. The $\nu_{C=O}$ at 1720 cm^{-1} in both cases could be readily attributed to the carbonyl stretching of the –COOH groups. The interaction between the surface and the carbon atom of the –COOH groups increased $\nu_{C=O}$ by withdrawing electron density from the carbon atom. The 1680 cm^{-1} band [also observed in *n*-butane oxidation and adsorption (Fig. 3 and Fig. 4), maleic anhydride adsorption at 100°C (Fig. 16), and crotonaldehyde adsorption at 300°C (Fig. 20)] was due to the interaction between the aldehyde group with coordinately unsaturated metal cations (Lewis acid sites). The metal cation could form a σ-complex with the carbonyl through sharing the lone electron pair of the carbonyl oxygen ($C{=}O: \rightarrow M^{n+}$); $\nu_{C=O}$ would therefore be lowered. This effect has been elaborated by Davydov using the example of acrolein oxidation (24). Maleic acid gas-phase dehydration produced a significant amount of maleic anhydride, which can adsorb on the catalyst, perhaps dissociatively, to form aldehyde functionalities. The aldehyde groups can coordinate with Lewis acid sites, and a carbonyl-stretching band at 1682 cm^{-1} results. Fumaric acid dehydration to maleic anhydride did not occur at low temperatures since its hydroxyl groups are *trans* to each other. Therefore, no surface aldehyde functionalities were formed upon adsorption and the only carbonyl stretching band observed was at 1720 cm^{-1} because of the –COOH groups.

These observations suggest that (a) fumaric acid and maleic acid can be converted to maleic anhydride in gas-phase, (b) the acids adsorb to form carboxylate species which decompose upon heating.

DISCUSSION

In the current study, *n*-butane adsorption on $(VO)_2P_2O_7$ was observed to produce unsaturated compounds at temperatures below 100°C. Gas-phase 1,3-butadiene could be detected, and the formation of other unsaturated compounds were indicated by a band near 1720 cm^{-1} and by a weaker band in the region of 1680–1660 cm^{-1} (Figs. 2 and 3). At higher temperatures, IR bands due to maleic anhydride (1850 and 1775 cm^{-1})[1] became significant. These species were detected at short time intervals under transient reaction conditions.

Important intermediates were associated with the appearance of a broad band near 1720 cm^{-1}. This band emerged in the n-C_4H_{10}/N_2 step and persisted in the O_2/N_2 step when bands due to gaseous compounds (e.g., 1,3-butadiene) disappeared (Fig. 3). The surface species associated with this band was formed before the detection of maleic anhydride, and it decreased in intensity as maleic anhydride was produced (Figs. 2–4). Therefore, the band near 1720 cm^{-1} was likely related to precursors to maleic anhydride. Busca and Centi (18) ascribed a band around 1715 cm^{-1} and a band at 1780 cm^{-1} to 2(5*H*)-furanone. However, the IR spectrum of 2(5*H*)-furanone has two bands at different positions, 1780 and 1740 cm^{-1}, and therefore this assignment is unlikely. Our studies of 2(5*H*)-furanone (Fig. 12) and γ-butyrolactone (Fig. 14) adsorption also indicated that these cyclic species were not stable on the catalyst surface: both compounds underwent ring cleavage upon adsorption. Wenig and Schrader assigned

[1] The 1850 cm^{-1} band is less intense than 1780 cm^{-1} band because the symmetric vibration of two carbonyl groups of maleic anhydride reduces the dipole moment (22). Based on our observation, this effect is more significant at higher temperatures: a decrease in the temperature increases the intensity of the 1850 cm^{-1} band.

the 1720 cm^{-1} band to maleic acid (10–12). The observation in our transient studies that this band emerged at room temperature before the formation of maleic anhydride discounts this assignment also.

The IR bands of carbonyl stretching modes for most noncyclic compounds such as ketones and aldehydes are in the region of 1750–1700 cm^{-1} (22–24, 27). The interaction of carbonyl groups with the catalyst may shift the positions of these bands, according to the different modes of adsorption. For instance, the carbonyl oxygen may form a hydrogen bond with surface hydroxyl groups (C=O $\cdots$ HO), or it may form a coordination bond with a surface cation (C=O $\cdots$ M^{n+}). This inductive effect increases the polarity of the C=O bond and makes it more ionic; a frequency shift to lower wavenumbers results (22, 24). On the other hand, if electron-withdrawing interactions occur through the carbon atom (electron-withdrawing group $\leftarrow$C=O), the polarity of the C=O bond is reduced, and the carbonyl frequencies will increase (22). The $\Delta\nu_{C=O}$ caused by such interactions is relatively small, and the $\nu_{C=O}$ of many aldehydes and ketones remains close to 1700 cm^{-1}. For instance, the carbonyl stretching band of surface formaldehyde species (24), adsorbed acrolein (24), products of propane partial oxidation (34), and the aldehydes and ketones involved in the current study are all in the region of 1750–1650 cm^{-1}. The carbonyl frequencies of strained ring compounds have unique features such as their occurrence at higher wavenumber positions and/or the presence of double carbonyl bands; these features distinguish these compounds from open chain species. For instance, Bellamy (22) showed that carbonyl frequencies of four or five-membered rings are usually higher than 1750 cm^{-1}. Also, 1,3-dicarbonyl compounds exhibit two carbonyl bands due to the symmetric and asymmetric vibration modes of the two carbonyl groups, as exemplified by maleic anhydride (bands at 1855 and 1784 cm^{-1}) and succinic anhydride (bands at 1876 and 1799 cm^{-1}). Some cyclic monocarbonyl compounds such as 2(5*H*)-furanone and cyclopentanone can exhibit split carbonyl bands as a result of Fermi resonance interactions. Based on this information about carbonyl stretching vibrations, therefore, the band near 1720 cm^{-1} can best be assigned to noncyclic carbonyl species.

Although not as intense as the 1720 cm^{-1} band, other bands near 1680 cm^{-1} were also observed for *n*-butane oxidation (Fig. 3). These bands indicate the presence of two types of surface complexes: the 1720 cm^{-1} band may be due to a species whose carbonyl carbon atom interacts with the catalyst surface (O=C $\cdots$ surface); the bands near 1680 cm^{-1} may be due to a species whose carbonyl oxygen interacts with Lewis acid sites (C=O $\cdots$ V^{4+}) or with surface hydroxyl groups (C=O $\cdots$ OH).

The adsorption studies of 2,5-dihydrofuran, furan, and 2(5*H*)-furanone verified that they can be oxidized to maleic anhydride on the VPO catalyst, as indicated by the presence of peaks at 1850 and 1780 cm^{-1}. However, in doing so, these compounds likely undergo ring cleavage first. Even at room temperature, the adsorption of these compounds on the catalyst resulted in ring opening: this was evidenced by the disappearance of ring vibration bands and the emergence of the noncyclic carbonyl stretching band near 1720 cm^{-1}. In contrast, ethyl methyl ketone, methyl vinyl ketone, butyraldehyde, and crotonaldehyde oxidation resulted in formation of maleic anhydride (1850 and 1775 cm^{-1}). No evidence for cyclic intermediates such as furan or 2(5*H*)-furanone was observed.

The aldehydes and ketones used in these adsorption studies still require two oxygen atoms to form maleic anhydride. However, 2(5*H*)-furanone is only "one oxygen away" from maleic anhydride and could be converted to maleic anhydride through an open chain intermediate. This surface species could therefore be involved in the reaction step just prior to the formation of maleic anhydride. Figure 24 provides several possible products of 2(5*H*)-furanone ring cleavage. Formation of many open chain compounds is

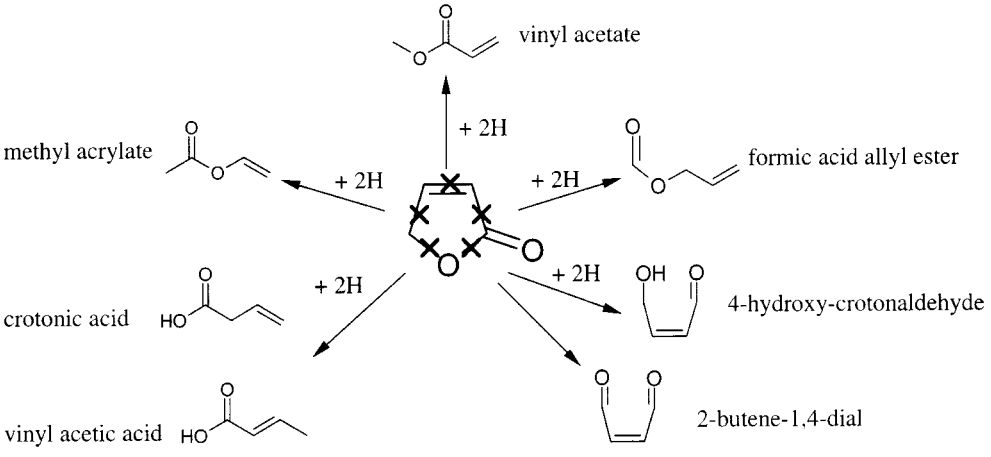

FIG. 24. Possible pathways of 2(5*H*)-furanone ring cleavage and resulting compounds.

possible: crotonic acid, methyl acrylate, vinyl acetate, vinyl acetic acid, 4-hydroxy-crotonaldehyde, 2-butene-1,4-dial, or formic acid allyl ester.

Adsorption of crotonic acid, vinyl acetic acid, vinyl acetate, and methyl acrylate on vanadyl pyrophosphate at 300°C did not produce bands for maleic anhydride. The RCO-OR′ bond is relatively reactive. Breaking of this bond will produce 4-hydroxy-crotonaldehyde or 2-butene-1,4-dial. The carbonyl stretching bands of these compounds are all near 1700 cm^{-1} (35, 36). Because of the reactivity of these aldehydes, it was not possible to purchase these compounds. The adsorption of their structural analog, 2-butene-1,4-diol, was performed, but dehydration occurred in the gas-phase to form crotonaldehyde. However, additional experimental evidence for this intermediate has been reported in the literature. Hönicke (37, 38) detected substantial amount of 2-butene-1,4-dial when investigating 1,3-butadiene partial oxidation on supported V_2O_5 catalysts, and it was suggested to be a precursor for maleic anhydride. In our reactor studies using mass spectrometry, a peak at $m/e = 84$ was detected for *n*-butane and 1,3-butadiene oxidation. Kubias *et al.* (5) also detected a peak at $m/e = 84$ in *n*-butane oxidation on VPO catalysts. They further showed that the compound corresponding to this peak contains two oxygen atoms since peaks at $m/e = 86$, 88 emerged upon O^{18} isotopic labeling. Additional evidence for the existence of such surface species has come from Crew and Madix (39) who studied furan oxidation to maleic anhydride on Ag(110). Using O^{18} labeling and temperature-programmed reaction spectroscopy (TPRS) experiments, it was found that the furan ring oxygen became one of the carbonyl oxygens of maleic anhydride product. They postulated that the furan ring opened to form an intermediate, specifically 2-butene-1,4-dial, and re-closed to form maleic anhydride. Based on these previous studies and the results of our new research, a noncyclic dialdehyde surface species structurally related to 2-butene-1,4-dial is proposed to be the direct precursor to maleic anhydride.

It should further be emphasized that the precursors to maleic anhydride are unsaturated compounds. The spectral bands 1620 cm^{-1} for C=C double bond near were always observed upon adsorption of the hydrocarbons, even if the adsorbates were saturated compounds (e.g., *n*-butane, ethyl methyl ketone, butyraldehyde). Moreover, the evolution of $\nu_{C=C}$ always paralleled that of the 1720 cm^{-1} band for $\nu_{C=O}$.

The results of IR studies of 1-butene oxidation on VPO catalysts agree well with these observations. The study conducted by Wenig and Schrader (11) showed that a band near 1725 cm^{-1} was in present together with bands at 1850, 1775, and 1615 cm^{-1}. Busca and Centi (18) observed the same bands in their study. Moreover, they showed that the 1715 cm^{-1} band was intense early in the adsorption when the 1850 and 1775 cm^{-1} were weak, and diminished after being heated in oxygen when the later bands dominated. By adsorbing 1-butene on an alumina supported VPO catalyst, Ramstetter and Baerns (16) observed the carbonyl stretching band at 1680 cm^{-1}. Puttock and Rochester (15) reported the isomerization of 1-butene to *trans* and *cis*-2-butenes on the surface of $(VO)_2P_2O_7$.

The adsorption of 1,3-butadiene on the catalyst at low temperatures did not show a band near 1720 cm^{-1}. Instead, it exhibited bands at 1550, 1490, and 1460 cm^{-1} which can be ascribed to adsorbed furan. However, the change in the relative intensities between the 1490 and 1460 cm^{-1} band suggested the formation of a furan complex whose α-position was attacked. A possible surface complex was proposed by Crew and Madix in their studies of furan oxidation (39). This complex may lead to ring cleavage to form 2-butene-1,4-dial. Oxidation of 1,3-butadiene at higher temperatures clearly exhibited a band at 1712 cm^{-1} which is consistent with the eventual conversion of this intermediate to maleic anhydride (Fig. 6).

The oxidation of *n*-butane and 1,3-butadiene on VPO catalysts are known to result in very different product distributions (4). The current study suggests that reason for this difference may be attributed the initial adsorption of these compounds. *n*-Butane adsorption and activation is likely a transformation largely related to hydrogen abstraction. It is possible that only active sites capable of hydrogen abstraction from *n*-butane are geometrically and energetically favorable for selective conversion of the adsorbed species to maleic anhydride. In contrast, 1,3-butadiene, due to its possession of double bonds, adsorbs strongly on the catalyst surface. Species adsorbed on selective sites will be converted to desired oxygenated products; other adsorbed species could be involved in side reactions such as oligomerization, isomerization, etc. Other workers have reported the

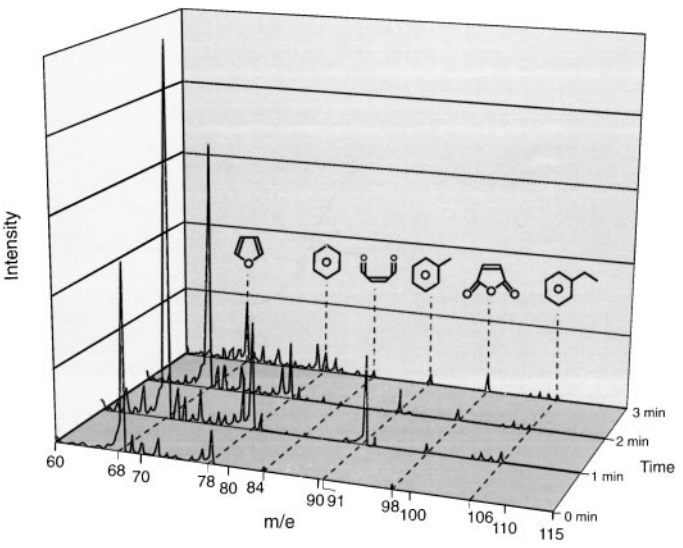

FIG. 25. Mass spectra of gas phase products during the 1,3-butadiene/N_2 step in reaction studies.

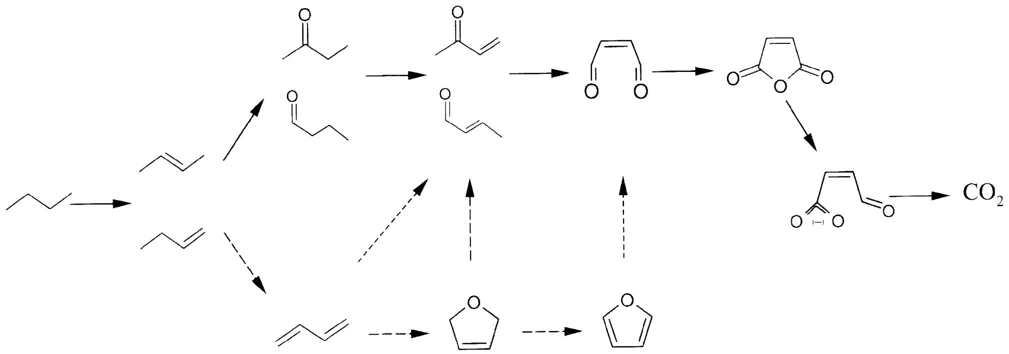

FIG. 26. Proposed reaction pathway for *n*-butane oxidation to maleic anhydride.

formation of several products for 1,3-butadiene oxidation. Centi and Trifirò (40) have observed maleic anhydride, furan, and crotonaldehyde for 1,3-butadiene oxidation on VPO. Hönicke (37) identified as many as 33 oxidation products in partial oxidation of 1,3-butadiene on supported V_2O_5 catalysts. The major products discovered in his study included maleic anhydride, phthalic anhydride, crotonaldehyde, furan, dihydrofurans, 2-butene-1,4-dial, and benzene derivatives.

Benzene derivatives can be produced form 1,3-butadiene dimerization (41). In our work, we monitored the reactor effluent for 1,3-butadiene oxidation over VPO catalysts at 300°C with mass spectrometry using a microreactor system. Intense peaks were observed at $m/e = 68$, 78, 91, and weak peaks were detected at $m/e = 82$, 84, 98, 106 (see Fig. 25). The peak at $m/e = 68$ is due to furan, $m/e = 98$ is due to maleic anhydride, $m/e = 78$ is due to benzene, and $m/e = 84$ may be attributed to 2-butene-1,4-dial. The peak at $m/e = 91$ is likely due to methylbenezene molecular ions, while the signal at $m/e = 106$ might be ascribed to ethylbenzene. Comparing the spectra collected at the first, second, and third minutes of a 1,3-butadiene/N_2 step (Fig. 25), signals from furan ($m/e = 68$), benzene ($m/e = 78$), and methylbenzene ($m/e = 91$) were intense at the beginning of the 1,3-butadiene step and decreased as the reaction proceeded; peaks due to maleic anhydride ($m/e = 98$) remained consistently low. This observation does not support the proposal that furan is a direct precursor to maleic anhydride.

The adsorption of maleic anhydride, maleic acid, and fumaric acid provided insights to the mechanism of maleic anhydride oxidation. The adsorption of all these species produced carboxylate species, which lead to the formation of carbon oxides (complete oxidation). The band at 1682 cm^{-1} evidenced the presence of aldehyde groups bound to Lewis acid sites corresponding to maleic anhydride oxidation. Lewis acid sites may play a role in maleic anhydride decomposition, for instance, by strongly anchoring the maleic anhydride molecules on the surface through the coordination bond: $C{=}O\cdots V^{4+}$.

CONCLUSION

$(VO)_2P_2O_7$ is sufficiently active to activate saturated C–H bonds at low temperatures, e.g. 50°C. Although formation of furan from 1,3-butadiene oxidation was observable and conversion of cyclic compounds to maleic anhydride cannot be completely excluded, the evidence from our transient IR and reactor studies indicates that: (a) the predominant surface species for *n*-butane oxidation are unsaturated noncyclic carbonyl compounds, and (b) these reactive surface species are the precursors to maleic anhydride. Based on these results and comparison with the literature, the reaction pathway shown in Fig. 26 can be proposed for *n*-butane partial oxidation to maleic anhydride.

This pathway suggests that for the main route for *n*-butane conversion to maleic anhydride, hydrogen abstraction occurs first to generate surface-bound olefinic compounds. Subsequent oxidation of these compounds forms unsaturated noncyclic carbonyl intermediates; formation of a noncyclic dialdehyde surface species appears likely. This surface species undergoes oxygen insertion and cyclization to form maleic anhydride. Complete combustion of intermediates or maleic anhydride involves carboxylate surface species which can be transformed to carbon oxides.

ACKNOWLEDGMENTS

The authors are grateful to K. Kourtakis at DuPont Central Research and Development for synthesis of the catalyst used in these studies. This work was conducted through the Ames Laboratory which is operated through the U.S. Department of Energy by Iowa State University under Contract W-7405-Eng-82. Support from the Office of Basic Energy Sciences, Chemical Sciences Division is also acknowledged.

REFERENCES

1. Hodnett, B. K., *Catal. Rev.-Sci. Eng.* **27**, 373 (1985).
2. Cavani, F., and Trifirò, F., *in* "Catalysis, Vol. 11," The Royal Society of Chemistry, London, 1994.
3. Albonetti, S., Cavani, F., and Trifirò, F., *Catal. Rev.-Sci. Eng.* **38**, 413 (1996).

4. Centi, G., Trifirò, F., Enber, J. R., and Franchetti, V. M., *Chem. Rev.* **88**, 55 (1988).
5. Kubias, B., Rodemerck, U., Zanthoff, H.-W., and Meisel, M., *Catal. Today* **32**, 243 (1996).
6. Zhang-Lin, Y., Forissier, M., Sneeden, R. P., Vèdrine, J. C., and Volta, J. C., *J. Catal.* **145**, 256 (1994).
7. Zhing-Lin, Y., Forissier, M., Vèdrine, J. C., and Volta, J. C., *J. Catal.* **145**, 267 (1994).
8. Ziólkowski, J., Bordes, E., and Courtine, P., *J. Catal.* **122**, 126 (1990).
9. Busca, G., *Catal. Today* **27**, 457 (1996).
10. Wenig, R. W., and Schrader, G. L., *J. Phys. Chem.* **90**, 6480 (1986).
11. Wenig, R. W., and Schrader, G. L., *J. Phys. Chem.* **91**, 1911 (1987).
12. Wenig, R. W., and Schrader, G. L., *J. Phys. Chem.* **91**, 5674 (1987).
13. Puttock, S. J., and Rochester, C. H., *J. Chem. Soc., Faraday Trans. 1* **82**, 2773 (1986).
14. Puttock, S. J., and Rochester, C. H., *J. Chem. Soc., Faraday Trans. 1* **82**, 3013 (1986).
15. Puttock, S. J., and Rochester, C. H., *J. Chem. Soc., Faraday Trans. 1* **82**, 3033 (1986).
16. Ramstetter, A., and Baerns, M., *J. Catal.* **109**, 303 (1988).
17. Do, N. T., and Baerns, M., *Appl. Catal.* **45**, 9 (1988).
18. Busca, G., and Centi, G., *J. Am. Chem. Soc.* **111**, 46 (1986).
19. Busca, G., Ramis, G., and Lorenzelli, V., *J. Mol. Catal.* **55**, 1 (1989).
20. Pekar, M., and Koubek, J., *Chem. Eng. Sci.* **52**, 2291 (1997).
21. Horowitz, H. S., Blackstone, C. M., Sleight, A. W., and Teufer, G., *Appl. Catal.* **38**, 193 (1988).
22. Bellamy, L. J., "The Infrared Spectra of Complex Molecules, 2nd ed. Vol. 2: Advances in Infrared Group Frequencies," Chapman & Hall, London, 1980.
23. Nakanishi, K., and Solomon, P. H., "Infrared Absorption Spectroscopy, Second Edition" Holden–Day, Oakland, CA, 1977.
24. Davydov, A. A., *in* "Infrared Spectroscopy of Adsorbed Species on the Surface of Transition Metal Oxides" (C. H. Rochester, Eds.), Wiley, New York, 1984.
25. Mckean, D. C., Mackenzie, M. W., Morrisson, A. R., Lavalley, J. C., Janin, A., Fawcett, V., and Edwards, H. G. M., *Spectrochim. Acta. A* **41**, 435 (1985).
26. Bondybey, V. E., and Nibler, J. W., *Spectrochim. Acta. A* **29**, 645 (1973).
27. Pouchert, C. J., "The Aldrich Library of FT-IR Spectra, Edition I, Vol 3," Aldrich Chemical, Co., 1989.
28. Mirone, P., and Chiorboli, P., *Spectrochim. Acta* **18**, 1425 (1962).
29. Klots, T. D., Chirico, R. D., and Steele, W. V., *Spectrochim. Acta. A* **50**, 765 (1994).
30. Rico, M., Barrachina, M., and Orza, J. M., *J. Mol. Spectrosc.* **24**, 133 (1967).
31. Klots, T. D., and Collier, W. B., *Spectrochim. Acta. A* **50**, 1725 (1994).
32. Jones, R. N., Angell, C. L., Ito, t., and Smith, R. J. D., *Can. J. Chem.* **37**, 2007 (1959).
33. Hargreaves, M. K., and Stevinson, E. A., *Spectrochim. Acta.* **21**, 1681 (1965).
34. Centi, G., Marchi, F., Perathoner, S., *J. Chem. Soc., Faraday Trans.* **92**(24), 5141 (1996).
35. Cyr, A., Wermeckes, B., and Beck, F., *J. Prakt. Chem.* **336**, 602 (1994).
36. Hufford, D. L., Tarbell, D. S., and Koszalka, T. R., *J. Amer. Chem. Soc.* **74**, 3014 (1952).
37. Hönicke, D., *J. Catal.* **105**, 10 (1987).
38. Hönicke, D., *J. Catal.* **105**, 19 (1987).
39. Crew, W. W., and Madix, R. J., *J. Am. Chem. Soc.* **115**, 729 (1993).
40. Centi, G., and Trifirò, F., *J. Mol. Catal.* **35**, 255 (1986).
41. Diesen, R. W., U.S. Patent: 5,276,257, assigned to The Dow Chemical Company, 1994.